Molecular and Cellular Endocrinology 400 (2015) 112–128

Contents lists available at ScienceDirect

Molecular and Cellular Endocrinology

journal homepage: www.elsevier.com/locate/mce

Nephrin, a transmembrane protein, is involved in pancreatic beta-cell survival signaling

Katerina Kapodistria [a], Effie-Photini Tsilibary [a], Panagiotis Politis [b], Petros Moustardas [c], Aristidis Charonis [c], Paraskevi Kitsiou [a,*]

[a] Institute of Biosciences and Applications, National Centre for Scientific Research, N.C.S.R. "Demokritos", Terma Patriarchou Grigoriou & Neapoleos, 15310 Agia Paraskevi, Attiki, Greece
[b] Center for Basic Research, Biomedical Research Foundation Academy of Athens (BRFAA), 4 Soranou Ephessiou, Athens 115 27, Greece
[c] Center for Clinical, Experimental Surgery and Translational Research, Biomedical Research Foundation Academy of Athens (BRFAA), 4 Soranou Ephessiou, Athens 115 27, Greece

ARTICLE INFO

Article history:
Received 13 May 2014
Received in revised form 15 October 2014
Accepted 3 November 2014
Available online 28 November 2014

Keywords:
Nephrin signaling
Pancreatic β-cells
PI3K-Akt survival signaling
High glucose
Nephrin internalization
Diabetic mouse pancreatic islets

ABSTRACT

Nephrin, a cell surface signaling receptor, regulates podocyte function in health and disease. We study the role of nephrin in β-cell survival signaling. We report that in mouse islet β-cells and the mouse pancreatic beta-cell line (βTC-6 cells) nephrin is associated and partly co-localized with PI3-kinase. Incubation of cells with functional anti-nephrin antibodies induced nephrin clustering at the plasma membrane, nephrin phosphorylation and recruitment of PI3-kinase to nephrin thus resulting in increased PI3K-dependent Akt phosphorylation and augmented phosphorylation/inhibition of pro-apoptotic Bad and FoxO. Nephrin silencing abolished Akt activation and increased susceptibility of cells to apoptosis. High glucose impaired nephrin signaling, increased nephrin internalization and up-regulated PKCα expression. Interestingly, a marked decrease in nephrin expression and phosphorylated Akt was observed in pancreatic islets of *db/db lepr−/−* diabetic mice. Our findings revealed that nephrin is involved in β-cell survival and suggest that glucose-induced changes in nephrin signaling may contribute to gradual pancreatic β-cell loss in type 2 diabetes.

1. Introduction

Nephrin was first identified in the slit diaphragm of renal glomerular epithelial cells (podocytes) (Kestila et al., 1998; Ruotsalainen et al., 1999; Tryggvason, 1999). Nephrin is a cell surface receptor of the immunoglobulin superfamily, participating in cell–cell adhesion and signaling functions (Huber and Benzing, 2005; Patrakka and Tryggvason, 2007). Through its extracellular IgG domains, nephrin can mediate *cis* and *trans* homophilic interactions with other nephrin molecules as well as with other slit diaphragm proteins from neighboring podocytes (Barletta et al., 2003; Khoshnoodi et al., 2003). Through its cytoplasmic tail, nephrin was shown to interact with CD2-associated protein (CD2AP) (Shih et al., 2001) and podocin in podocytes (Boute et al., 2000). These interactions linking the slit diaphragm-associated protein complex to actin cytoskeleton (Yuan et al., 2002) maintain structural and functional integrity of the glomerular filtration barrier and also facilitate nephrin downstream signaling (Huber et al., 2001, 2003b; Schwarz et al., 2001). Nephrin engagement in homophilic and heterophilic interactions results in the modulation of nephrin-dependent signaling (Heikkila et al., 2011). This function of nephrin is enabled by nine tyrosine residues located in the intracellular domain, which become phosphorylated by specific kinases of the Src family, including Fyn (Lahdenpera et al., 2003; Verma et al., 2003). An important role of nephrin phosphorylation in governing actin dynamics and lamellipodia formation (George et al., 2012; Venkatareddy et al., 2011) has been recently reported in podocytes. Upon homophilic or heterophilic interactions, tyrosine phosphorylation of nephrin controls the interaction of nephrin with the SH2–SH3 domain-containing adaptor proteins Nck1 and Nck2 (Jones et al., 2006; Verma et al., 2006) and with phosphoinositide 3-OH kinase (PI3K) (Huber et al., 2003a; Simons et al., 2001; Zhu et al., 2008); this signaling cascade regulates actin polymerization, cell survival and cellular morphology in podocytes (Tryggvason et al., 2006). Subsequently, the expression of nephrin and several nephrin-associated proteins were reported in pancreatic beta-cells (Palmen et al., 2001; Rinta-Valkama et al., 2007), where their function remains largely

* Corresponding author. Institute of Biosciences and Applications, National Centre for Scientific Research "Demokritos", Terma Patriarchou Grigoriou & Neapoleos, 15310 Agia Paraskevi, Attiki, Greece. Tel.: +30 210 6503615, +30 210 6503573; fax: +30 210 6511767.
E-mail address: pkit@bio.demokritos.gr (P. Kitsiou).

http://dx.doi.org/10.1016/j.mce.2014.11.003

unknown. Recently, Fornoni et al. (2010) demonstrated that nephrin is an active component of the insulin vesicle machinery affecting vesicle–actin interactions and vesicle mobilization to the cell surface. Dynamin-dependent nephrin phosphorylation occurs in response to glucose and is necessary for nephrin-mediated augmentation of glucose-stimulated insulin release (GSIR) in pancreatic beta-cells (Jeon et al., 2012).

In the present study, we investigated the potential role of nephrin in pancreatic beta-cell survival. We demonstrated that nephrin was associated with PI3-kinase and CD2AP in both mouse islet β-cells and the mouse pancreatic β-cell line (βTC-6 cells). We showed that nephrin homophilic interactions triggered PI3-kinase-dependent Akt survival signaling in cultured βTC-6 cells. Moreover, we provided evidence that increased glucose concentrations impaired nephrin signaling and/or expression in both βTC-6 cells and pancreatic islets of diabetic mice. Our data suggest that glucose-induced changes in nephrin signaling may contribute to gradual pancreatic β-cell loss which occurs in type 2 diabetes.

2. Materials and methods

2.1. Antibodies and reagents

Goat polyclonal anti-nephrin C17 (Cat. No: sc-32529), anti-nephrin N20 (Cat. No: sc-19000), mouse monoclonal anti-CD2AP (Cat. No: sc-25272), goat polyclonal anti-podocin (Cat. No: sc-22294), rabbit polyclonal anti-phospho-Ser136 Bad (Cat. No: sc-7999-R), rabbit polyclonal anti-Bad (Cat. No: sc-942), donkey anti-goat IgG F(ab)$_2$ fragment (Cat. No: sc-3850) and mouse monoclonal anti-PKCα (Cat. No: sc-8393) antibodies were purchased from Santa Cruz Biotechnology, Inc. Rabbit monoclonal anti-nephrin (phospho Y1176 + Y1193) antibody [EPTPG1] (Cat. No: ab-80299) was purchased from Abcam. Rabbit monoclonal anti-p85α/PI3 kinase antibody (Cat. No: 04–403) was purchased from Millipore. Rabbit polyclonal anti-Akt (Cat. No: 9272), rabbit monoclonal anti-phospho-Ser473 Akt (Cat. No: 40605), rabbit polyclonal anti-phospho-FoxO1(Thr24)/FoxO3a(Thr32) (Cat. No: 9464), rabbit polyclonal anti-cleaved caspase-3 (Cat. No: 9661) and anti-PARP (Cat. No: 9542) antibodies were purchased from Cell Signaling. Rabbit polyclonal anti-ZO-1 antibody (Cat. No: 61-7300) was purchased from Invitrogen. Mouse monoclonal anti-insulin antibody (Cat. No: I 2018) was purchased from Sigma. Fluorescent secondary antibodies, donkey anti-rabbit Alexa Fluor 594 (Cat. No: A-21207), donkey anti-goat Alexa Fluor 488 (Cat. No: A-11055), donkey anti-mouse Alexa Fluor 594 (Cat. No: A-21203) and donkey anti-mouse Alexa Fluor 488 (Cat. No: A-21202), were purchased from Molecular Probes, Invitrogen. PI3K inhibitors, wortmannin (#9951) and LY294002 (#9901) were purchased from Cell Signaling. The Src kinases inhibitor PP1 was obtained from Enzo Lifes Sciences.

2.2. Cell line and culture conditions

Beta TC-6 cells, a mouse T-SV40 immortalized insulin secreting pancreatic beta-cell line (ATCC, Cat. No. CRL 11506) (Poitout et al., 1995), were continuously grown in DMEM culture medium containing 1 mmol.l^{-1} glucose (optimal glucose concentration for retention of glucose responsiveness and insulin secretion) (Poitout et al., 1996), 15 % (v/v) FCS, 4 mmol.l^{-1} glutamine, and antibiotics in 5% CO_2 at 37 °C. Medium was changed every 24 h, with fresh culture medium and cells sub-cultured as necessary to prevent over-confluence. Cells, which form islet-like clusters (pseudo-islets) in culture, were released from their tissue culture flasks for passaging by treatment with 0.25% (w/v) trypsin/0.03% (w/v) EDTA. For experiments, cells were used at passages 26–35.

2.3. Nephrin clustering

Clustering of nephrin was induced as previously described with some modifications (Aoyama et al., 2006; Lahdenpera et al., 2003; Liu et al., 2004). Briefly, βTC-6 cells, cultured in 24-well plates or grown on glass coverslips in the presence of 1 mmol.l^{-1} glucose, were washed with PBS and incubated with Kreb's Hepes buffer (118.5 mmol.l^{-1} NaCl, 2.54 mmol.l^{-1} $CaCl_2 2H_2O$, 1.19 mmol.l^{-1} KH_2PO_4, 4.74 mmol.l^{-1} KCl, 25 mmol.l^{-1} $NaHCO_2$, 1.19 mmol.l^{-1} $MgSO_4 7H_2O$, 10 mmol.l^{-1} Hepes buffer, 0.1% (w/v) BSA, pH 7.4) for 60 min (2 × 30 min) at 37 °C, to minimize phosphorylation of Akt induced by autocrine and paracrine-insulin signaling. Cells were then washed with ice-cold Kreb's buffer and incubated with 10 μg/ml goat anti-nephrin N-20 antibody (recognizes the extracellular Ig-like motifs 1–2 of nephrin) in Kreb's buffer, for 30 min on ice and sequentially with 10 μg/ml anti-goat IgG F(ab)$_2$ fragment in Kreb's buffer, for 15 min at 37 °C. Cells were then washed with ice-cold PBS, lysed and assessed using Western blotting analysis or fixed with paraformaldehyde and processed for immunofluorescence microscopy (see Section 2.4). Briefly, cells were incubated with anti-nephrin C-17 antibody (recognizes the cytoplasmic tail of nephrin) overnight at 4 °C and finally with the appropriate fluorescent secondary antibody for 1 hour at room temperature. Finally, coverslips were incubated with DAPI (0.7 μg/ml) in PBS for 5 min, and washed with PBS before mounting them with Dako Fluorescent Mounting Medium (Cat. No: S3023, Dako). Specimens were examined with a confocal laser-scanning microscope (TCS SP5 Confocal System, LEICA). Images were obtained and processed with Adobe Photoshop CS4 version 11.0, software. Analysis of the size of nephrin clusters was performed in digital images using MacBiophotonics Image J software; Application:Analyze Particles).

2.4. Immunocytochemistry and fluorescence labeling of βTC-6 cells

Beta TC-6 cells grown on glass coverslips were fixed with 4% (w/v) paraformaldehyde in PBS pH 7.4, for 15 min at room temperature. After 10 min quenching with 50 mmol.l^{-1} NH_4Cl, cells were permeabilized with 0.25% (v/v) Triton X-100 in PBS for 10 min, washed with PBS and blocked with 1% (w/v) BSA in PBS for 60 min at room temperature. Cells were then incubated with anti-nephrin C-17 antibody (recognizes the cytoplasmic tail of nephrin) and anti-p85α/PI3 kinase antibody or anti-CD2AP antibody overnight at 4 °C and finally with the appropriate fluorescent secondary antibodies for 1 hour at room temperature [all antibodies in PBS containing 1% (w/v) BSA]. Finally, coverslips were washed with PBS, incubated with DAPI (0.7 μg/ml) in PBS for 5 min, and washed again with PBS before mounting them with Dako Fluorescent Mounting Medium (Cat. No: S3023, Dako). Fluorescent specimens were examined with a confocal laser-scanning microscope (TCS SP5 Confocal System, LEICA). Images were obtained and processed with Adobe Photoshop CS4 version 11.0, software. Confirmation of nephrin–PI3K co-localization was performed in digital images using MacBiophotonics Image J software; Plugin: Colocalization Analysis-Intensity Correlation Analysis and Colocalization Threshold).

2.5. In vivo *analysis of nephrin and pAkt-fluorescence labeling of formalin-fixed paraffin-embedded (FFPE) tissue*

The well-established mouse model of *db/db* was used to evaluate the effect of high glucose on nephrin expression and Akt phosphorylation in *in vivo* studies. Animals (C57BLK) were purchased from Harlan and euthanized at the 10th wk after birth. The use of animal experimental protocols was approved by the Ethics Committee of the Biomedical Research Foundation Academy of Athens (BRFAA). Five animals were used as experimental diabetic model (*db/db* lepr−/−), and five animals were used as control

(db/db lepr+/–). Pancreata were isolated and fixed in 10% neutral buffered formalin overnight and then embedded into paraffin wax. Dual immunofluorescence labeling of FFPE pancreatic tissue sections from mice, for nephrin or Ser 473 pAkt and insulin was performed as previously described (Robertson et al., 2008). Briefly, 4–5 μm sections were cut from the embedded blocks and slides were de-waxed as follows: twice in 100% xylene for 5 minutes, 100% ethanol for 10–20 s, once in 90% ethanol for 10–20 s, once in 70% ethanol for 10–20 s and twice in H_2O for 10–20 s. Antigen retrieval was performed in pre-warmed (94 °C–96 °C) Dako target retrieval solution (S1699), for 30 minutes in a water bath (at 95 °C), 20 minutes on the bench and 5 minutes in running water. Slides were blocked with immunofluorescence buffer (IFF) (PBS plus 1% bovine serum albumin and 2% fetal calf serum) for 1 hour at RT. Slides were then incubated with primary antibodies diluted in IFF, overnight at 4 °C, washed (3 × 5 minute washes) in PBS and finally incubated with the appropriate fluorescent secondary antibodies (Molecular Probes) diluted in IFF for 1 hour at room temperature. Slides were washed with PBS, before mounting them with Dako Fluorescent Mounting Medium. Fluorescent specimens were examined with a confocal laser-scanning microscope (Bio-Rad). Images were obtained and processed with Adobe Photoshop CS4 version 11.0, software. Quantification of nephrin expression and pAkt levels was performed in digital images. From each group (five animals/group), 20–30 islets from random non-coincident fields were captured. Nephrin or pAkt fluorescence intensity was quantified in images using the Image J 1.43u image-processing and analysis software (National Institutes of Health). Briefly, Image J was used to quantify the fluorescence intensity and the area of each islet.

2.6. In situ *cell death detection – TUNEL staining*

Beta TC-6 cells grown on glass coverslips were fixed with 4% (w/v) paraformaldehyde in PBS pH 7.4, for 1 hour at room temperature, permeabilized for 2 min on ice with 0.1% TritonX-100 in 0.1% sodium citrate and finally incubated with 50 μl TUNEL reaction mixture (TdT enzyme and fluorochrome labeling solution) for 1 hour at 37 °C in the dark [*In Situ* Cell Death Detection Kit, TMR red (Roche Diagnostics, Mannheim, Germany)]. Finally, the cells were washed with PBS, and incubated with DAPI (1 μg/ml) in PBS for 5 min, before mounting with Dako Fluorescent Mounting Medium (Cat. No: S3023, Dako). Specimens were examined with a confocal laser-scanning microscope (TCS SP5 Confocal System, Leica). Images were obtained and processed with Adobe Photoshop CS4 version 11.0, software. Quantification of the percentage of cells undergoing apoptosis was performed in digital images.

2.7. *Western blotting and immunoprecipitation*

For Western blotting, following appropriate treatment where applicable, cells were lysed in Hepes lysis buffer [100 mmol.l^{-1} NaCl, 1% (v/v) Triton-X-100, 0.5% (w/v) sodium deoxycholate, 0.2% (w/v) SDS, 2 mmol.l^{-1} Na_2EDTA, 10 mmol/l^{-1} Hepes buffer (pH 7.5), 1xPhosSTOP (cocktail of phosphatase inhibitors, Roche) and 1xProtease inhibitors cocktail (Roche)]. Protein concentration was determined by the Bradford colorimetric assay (Pierce). Immunoblot analysis of cell lysates was performed as previously described (Kitsiou et al., 2003). To ensure equal amounts of protein loading, the blots were stripped (Re-Blot Plus Mild Solution, Cat. No: 2502, Millipore) and re-probed with anti-β-tubulin monoclonal antibody (Cat. No: T4026, Sigma). Immunoprecipitation of nephrin and nephrin-associated proteins from cell lysates was performed as previously described (Kitsiou et al., 2003). Briefly, 600 μg of total protein from cell lysate was incubated overnight at 4 °C with anti-nephrin N20 antibody. Immune complexes were captured with Protein G PLUS-Agarose (Cat. No: sc-2002, Santa Cruz) for 2 hours at 4 °C, followed by three washes in ice-cold PBS. Immune complexes were extracted with 60 μl boiling 2xLaemmli sample buffer containing 100 mmol.l^{-1} DTT. Fifty microliters of each supernatant fraction was processed for Western blot analysis.

2.8. *Transient small interfering (si)RNA transfection*

Prevalidated siRNAs targeting mouse nephrin (Cat. No: sc-36031, Santa Cruz Biotechnology, Inc.), a control, non-targeting siRNA (Cat. No: sc-37007, Santa Cruz Biotechnology, Inc.), transfection reagent, Lipofectamine RNAiMAX (Cat. No: P/N 56531, Invitrogen) and transfection medium OPTI-MEM I (Cat. No: 31985, Gibco) were used. Beta TC-6 cells growing in the presence of 1 mmol.l^{-1} glucose in medium in the absence of antibiotics were reverse transfected with 100 nmol/l^{-1} nephrin or control (scramble) siRNAs according to the manufacturer's instructions. Briefly, siRNAs–transfection reagent complexes in transfection medium were prepared inside the wells of a 24-well plate and incubated for 20 min at RT. Cells suspended in complete medium without antibiotics were then added to each well (7×10^4 cells/well) and incubated for 24 hours at 37 °C in a CO_2 incubator. Transfection medium was then replaced by complete medium without antibiotics. After 72 hours, media were removed, 100 nmol/l^{-1} nephrin or control (scramble) siRNAs were re-added (forward transfection), cells incubated for 24 hours at 37 °C in a CO_2 incubator and transfection medium was then replaced by complete medium without antibiotics. After 48 hours, cells were incubated with Kreb's Hepes buffer for 60 min (2 × 30 min) at 37 °C, to minimize phosphorylation of Akt induced by autocrine and paracrine-insulin signaling. Nephrin clustering was then induced, as previously described, and nephrin suppression and Akt phosphorylation were assessed using Western blotting analysis.

2.9. *Statistical analysis*

Values are presented as means ± SD. Statistically significant differences between values were evaluated by one-way ANOVA as appropriate. A $p < 0.05$ was considered statistically significant. Statistical analysis of the results from the sections of the *db/db* animals and their controls was also performed by Mann–Whitney nonparametric test.

3. Results

3.1. *Nephrin is expressed in the mouse insulin-secreting pancreatic βTC-6 cells and* in situ*, in mouse islet β-cells and associates with the p85 regulatory subunit of PI3K and CD2AP*

Western blot analysis demonstrated that cultured pancreatic βTC-6 cells express nephrin, CD2AP, podocin and ZO-1 proteins (Fig. 1A, see also Supplementary file 1). Co-immunoprecipitation experiments with nephrin-specific antibodies showed that endogenous nephrin was associated with the p85α regulatory subunit of PI3K and CD2AP in these cells (Fig. 1B). Dual-immunofluorescence confocal microscopy in βTC-6 cells confirmed that nephrin partly co-localized with PI3K and CD2AP (Fig. 1C). The association of nephrin with the p85 regulatory subunit of PI3K or CD2AP was also examined in mouse pancreatic islets. Immunofluorescence co-localization studies with nephrin and insulin or nephrin and $p85\alpha^{PI3K}$ in normal mice (db/db lepr+/–) pancreatic sections showed that nephrin expression occurs in β-cells (Fig. 1D, panel a and Fig. 9A) and moreover nephrin is partially co-localized with $p85\alpha^{PI3K}$ (Fig. 1D, panels a–d). Interestingly, staining of $p85\alpha^{PI3K}$ in pancreatic sections showed that $p85\alpha^{PI3K}$ was almost exclusively localized in islets whereas in pancreatic acinar cells, it was hardly detected (Fig. 1D, panel b). This finding is in agreement with a recent study which demonstrated

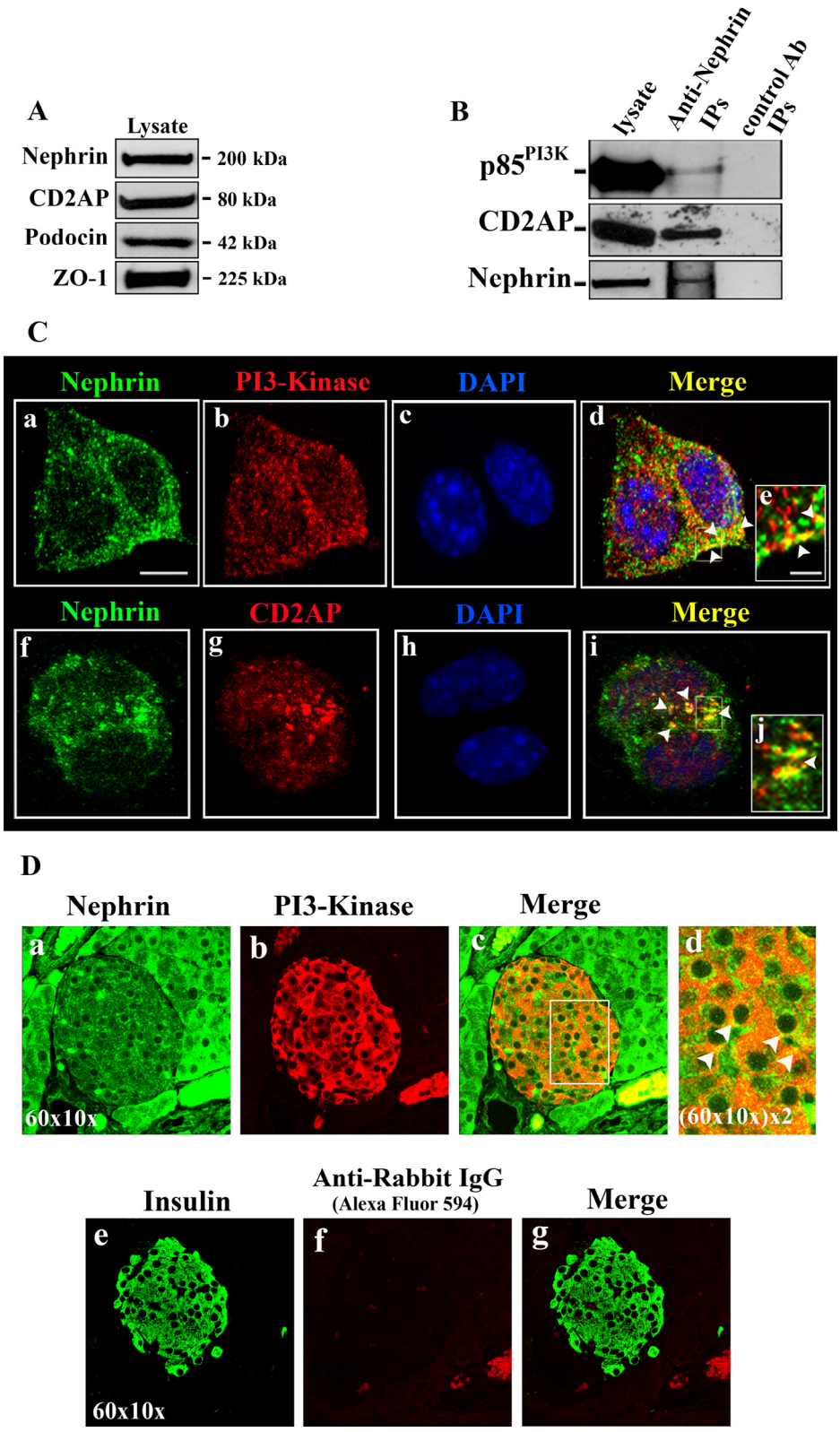

low levels of mouse exocrine pancreatic expression of p85α[PI3K], compared to islet p85α[PI3K] expression (Takahashi et al., 2012). However, other isoforms such as p85β[PI3K] and p85γ[PI3K], which are also expressed by acinar cells, can transduce through Akt activation, signaling which regulates acinar cell functions, including metabolism, proliferation and survival (Takahashi et al., 2012; Williams, 2010). To distinguish islet cells from acinar cells in the pancreas, a serial section (which corresponds to the section presented in panels a–c) was stained with an insulin-specific antibody (green) and the secondary antibody anti-rabbit IgG-Alexa Fluor 594 (red) alone (negative control) (Fig. 1D, panels e–g). Negative controls for the specificity of nephrin staining were included in Fig. 9A. Furthermore, we detected extensive co-localization of nephrin with CD2AP in both islets and exocrine pancreatic tissue (Supplementary file 2).

Taken together our data demonstrated that nephrin may participate in PI3K-mediated signaling in pancreatic β-cells.

3.2. Nephrin clustering recruited PI3K to nephrin

Nephrin clustering in podocytes is a prerequisite for nephrin signaling which can be experimentally induced by anti-nephrin antibodies (Lahdenpera et al., 2003). To further investigate the interaction between nephrin and PI3K, we used a model system to assess the effect of nephrin–ligand binding on nephrin signaling (Jones et al., 2006; Lahdenpera et al., 2003; Verma et al., 2006). More specifically, clustering of nephrin was induced on the surface of βTC-6 cells with the N20 antibody raised against a peptide (amino acids 64–83 of human nephrin) which maps near the N-terminus of human nephrin (Komori et al., 2008), at the extra cellular Ig 1–2 like motif of nephrin (Fig. 2A). N20 was used since nephrin clustering could be induced by antibodies that recognize the Ig-like motifs 1–2, 1–8 as well as full-length nephrin (Aoyama et al., 2006). Cells cultured on glass coverslips were incubated with "clustering" antibodies (as described in Section 2.3), fixed, permeabilized and stained with anti-nephrin C17 antibody (which recognizes nephrin cytoplasmic domain) and an appropriate Alexa-Flour secondary antibody. This treatment resulted in extensive aggregation (clustering) of nephrin (Fig. 2B, lower panel) with a ring-like appearance. Smaller aggregates also appeared when only N20 antibody was added to cells before fixation (Fig. 2B, middle panel). The addition of only secondary antibody (control) had no significant effect on nephrin localization (Fig. 2B, upper panel). Morphometric analysis of clusters revealed that the addition of both "clustering" antibodies induced a fourfold increase in the size of nephrin clusters (Fig. 2C) compared to control cells (cells incubated in the presence of secondary antibody only). In addition, the presence of N20 antibody alone resulted in a 2.5-fold increase of the size of nephrin clusters (Fig. 2C).

To examine whether nephrin clustering induces PI3K relocalization, βTC-6 cells were treated with "clustering" antibodies as described earlier, fixed, permeabilized, stained for nephrin (anti-nephrin C17 antibody which recognizes nephrin cytoplasmic domain was used) and p85α^{PI3K} and examined by confocal immunofluorescence microscopy. Clustering of nephrin at the cell surface resulted in considerable recruitment of PI3K to clustered nephrin, as indicated by substantially increased co-localization of nephrin with p85α^{PI3K} adjacent to the intracellular side of the plasma membrane (Fig. 3A, panels D-d). There were few PI3K-nephrin clusters in the absence or presence of only secondary or only primary "clustering" antibodies (Fig. 3A, panels A-a, B-b, C-c respectively). In addition, the presence of both "clustering antibodies" induced a fourfold increase in the number of cells which were positive to nephrin-PI3K co-localization compared to untreated cells or cells treated with primary or secondary antibody only (Fig. 3B). These results strongly support a role for nephrin clustering in the recruitment of PI3K to nephrin.

3.3. Clustering of nephrin activated PI3K-dependent Akt signaling

We next examined whether nephrin clustering can trigger PI3K-dependent Akt signaling. Figure 4A,B demonstrates that when cells were treated with "clustering" antibodies, nephrin clustering resulted in threefold increase of Ser473 Akt phosphorylation compared to untreated cells. The addition of only primary or only secondary antibody had no significant effect on Ser473 Akt phosphorylation. Nephrin-induced Akt phosphorylation was completely inhibited by the PI3K inhibitors wortmannin and LY294002, demonstrating that phosphorylation of Akt is PI3K-dependent (Fig. 4A,B). To confirm nephrin-mediated Akt activity, we monitored the extent of phosphorylation of Bad and FoxO1/FoxO3a (Forkhead box O family) transcription factors, both being proapoptotic elements, whose activity was suppressed by Akt-mediated phosphorylation at Ser 136 and Thr24/32 respectively (Hemmings and Restuccia, 2012). Cells were incubated with "clustering" antibodies (anti-nephrin N20: 30 min on ice, secondary antibody IgG [F(ab)$_2$ fragment]: 30 min at 37 °C), and lysed. Western blotting analysis demonstrated that clustering of nephrin also resulted in a significant increase of both Bad and FoxO phosphorylation/inhibition (11 ± 0.951) and (5.13 ± 0.430) respectively, compared to untreated cells (1 ± 0.000) (Fig. 4C,D). Nephrin-induced Bad and FoxO suppression was completely inhibited by the PI3K inhibitor wortmannin demonstrating that their phosphorylation is PI3K-dependent (Fig. 4C,D). In addition, the primary antibody alone also induced phosphorylation of Bad (4.36 ± 0.598) and FoxO (2.998 ± 0.226); however, the extent of phosphorylation was considerably lower compared to that observed in the presence of both "clustering" antibodies (Fig. 4C,D). These results indicated that nephrin-induced PI3K-Akt activation triggered anti-apoptotic signaling, in part via inhibition of Bad and FoxO1/FoxO3a activity.

3.4. Clustering-induced nephrin tyrosine phosphorylation and signaling were inhibited by PP1, a selective inhibitor of Src kinases

Cells growing in glass coverslips or in 24-well plates were pretreated or not for 1 hour with 10–20 μmol/l^{-1} PP1 (an inhibitor of Src kinases involved in nephrin phosphorylation), incubated with "clustering antibodies" (anti-nephrin N20: 30 min on ice; secondary antibody IgG [F(ab)$_2$ fragment]: 2–15 min at 37 °C, for nephrin phosphorylation experiments or 15 min at 37 °C, for PI3K recruitment and Akt phosphorylation experiments), in the presence or absence of PP1, fixed, permeabilized and stained for nephrin and p85α^{PI3K,} or lysed and nephrin tyrosine phosphorylation and Akt

Fig. 1. Nephrin interacted and partly co-localized with PI3K and CD2AP. Beta TC-6 cells grown in DMEM in the presence of 1 mmol.l^{-1} glucose were lysed and cell lysates were immunoblotted with anti-nephrin, anti-CD2AP, anti-podocin or anti-ZO-1 specific antibodies. (A) Representative Western blots from five independent experiments demonstrated that mouse pancreatic βTC-6 cells express nephrin and several nephrin-associated proteins. (B) Beta TC-6 cells cultured in the presence of 1 mmol.l^{-1} glucose were lysed and total protein was immunoprecipitated with anti-nephrin N20 antibody or control polyclonal antibody. Co-precipitating PI3K and CD2AP were detected with an anti-p85α^{PI3K} and anti-CD2AP-specific monoclonal antibodies. Representative Western blots from three independent experiments demonstrating the protein content of immunoprecipitates. (C) Cells grown on glass coverslips in DMEM were fixed and processed for immunocytochemistry as described in Section 2. Cells were stained with anti-nephrin C17 antibody (recognizes the cytoplasmic tail of nephrin) and anti- p85α^{PI3K} or anti-CD2AP antibodies and the appropriate secondary Alexa-Fuor antibodies. Nuclei were counterstained with DAPI. Three independent experiments were performed. Representative confocal images of βTC-6 cells stained (a–e) for nephrin cytoplasmic domain (green) and PI3K (red); (f–j) nephrin cytoplasmic domain (green) and CD2AP (red). (d) Low magnification and (e) high magnification of the selected area (white square) in (d) with nephrin-PI3K co-localization (white arrowheads). (i) Low magnification and (j) high magnification of the selected area (white square) in (i) with nephrin–CD2AP co-localization (white arrowheads). Scale bar in (a–d,f–i):10 μm and in (e–j): 2 μm. Secondary antibodies alone gave no signal (data not shown). Dual-immunofluorescence in specimens was viewed with a Leica confocal laser-scanning microscope. (D) Nephrin, PI3K and insulin were detected by fluorescence immunohistochemistry in sections of formalin-fixed paraffin-embedded murine pancreata from C57BL/KsJ *db/db (lepr +/–)* mice. Sections from three animals were examined. Representative confocal images of mouse pancreas section stained (a–c) for nephrin (green) and p85α^{PI3K} (red); (d) High magnification of the selected area (white square) in (c) with nephrin-PI3K co-localization (white arrowheads). To distinguish islet cells from acinar cells in the pancreas, a serial section (e–g) (which corresponds to section presented in panels a–c) was stained for insulin (green) and the secondary antibody anti-rabbit IgG-Alexa Fluor 594 (red) alone. Magnification: ×600. Dual-immunofluorescence in specimens was viewed with a BIORAD confocal laser-scanning microscope. (For interpretation of the references to color in this figure legend, the reader is referred to the web version of this article.)

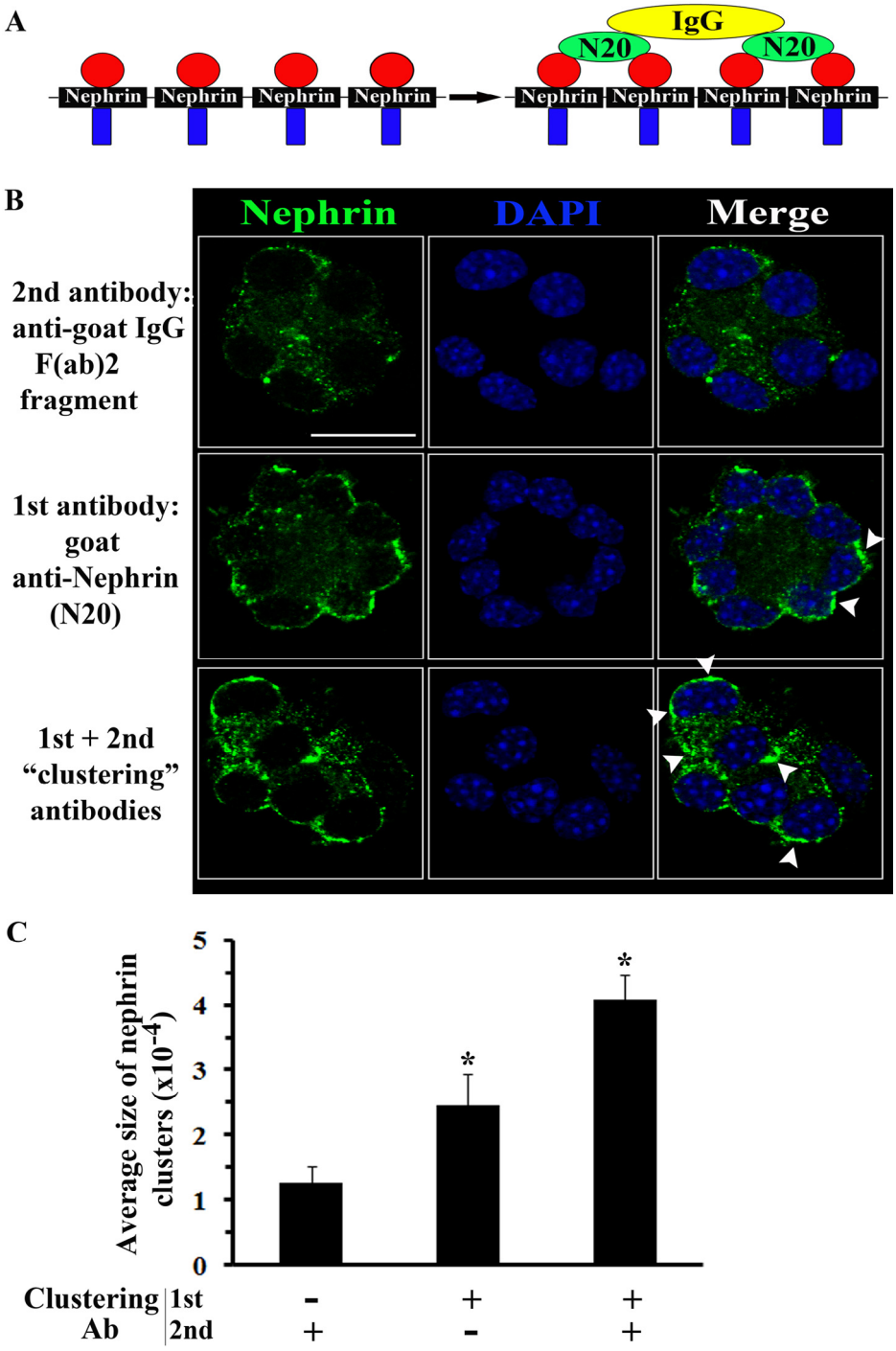

Fig. 2. Clustering of nephrin at the plasma membrane. (A) Schematic representation of the induction of nephrin clustering by antibodies. (B) Representative confocal images of nephrin clustering in βTC-6 cells. Beta TC-6 cells grown on glass coverslips in the presence of 1 mmol.l^{-1} glucose were incubated with "clustering" antibodies; the goat anti-nephrin N-20 antibody (recognizes the extracellular Ig-like 1–2 domain of nephrin) was added to cells for 30 min on ice and a secondary anti-goat IgG antibody [F(ab)$_2$ fragment] was then added for 15 min at 37 °C. Cells were fixed, permeabilized and stained with anti-nephrin C17 antibody (recognizes the cytoplasmic tail of nephrin) and the appropriate secondary Alexa-Fluor antibody (green). Nuclei were counterstained with DAPI. Images are representative from three independent experiments. White arrowheads illustrate regions of increased nephrin clustering. Scale bar: 20 μm. Secondary antibody alone gave no signal (data not shown). (C) Bar graph analysis of the size of clusters. Morphometric analysis of clusters was performed in digital images. In each case, a total of fifty cells from three independent experiments, with imaging of 5–10 cells each, were used to analyze the size of nephrin clusters, using *MacBiophotonics Image J software; Application: Analyze Particles.* Data represent the means ± SD; $n = 3$, $^*P < 0.05$ as compared to the size of clusters in cells incubated with the secondary antibody [F(ab)$_2$ fragment] only. (For interpretation of the references to color in this figure legend, the reader is referred to the web version of this article.)

phosphorylation were assessed by Western blotting. Nephrin clustering induced strong and immediate increase in phosphorylation of 1176 and/or 1193 tyrosine residues of nephrin; stimulated phosphorylation reached the highest levels between 2 and 5 min, and then decreased to basal levels (Fig. 5A). Phosphorylation of additional tyrosine residues in nephrin is also possible. Since Src kinases are known to be involved in tyrosine phoshorylation of nephrin (Lahdenpera et al., 2003; Verma et al., 2003), the effect of PP1

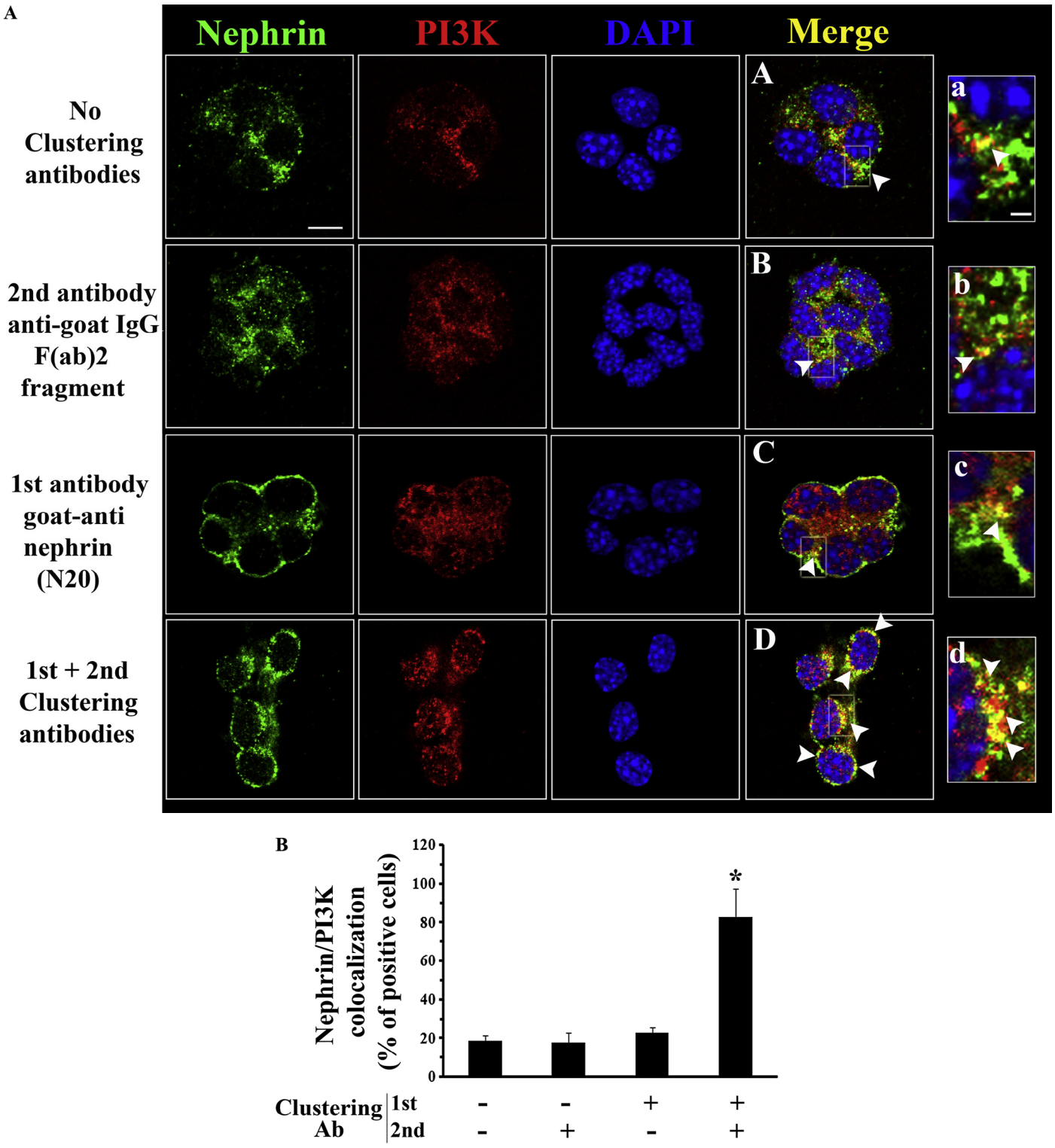

Fig. 3. Clustering of nephrin at the plasma membrane recruited PI3K to nephrin. Cells grown on glass coverslips were incubated in the presence or absence of "clustering" antibodies as described in Fig. 2. Cells were then fixed, permeabilized, stained with anti-nephrin C-17 antibody (recognizes the cytoplasmic tail of nephrin) and anti-p85α^{PI3K} mAb, and in sequence with the appropriate secondary Alexa-Fluor antibodies. Nuclei were counterstained with DAPI. Three independent experiments were performed. (A) Representative confocal images of βTC-6 cells stained for nephrin cytoplasmic domain (green) and PI3K (red). (A–D) Low magnification and (a–d) high magnification of the selected areas (white squares) in (A–D) respectively, with nephrin–PI3K co-localization (white arrowheads). In the presence of both "clustering antibodies", nephrin–PI3K co-localization was significantly increased (panels D, d) compared to cells incubated in the absence of clustering antibodies (panels A, a) or in the presence of secondary antibody only (panels B, b) or in the presence of primary antibody only (panels C, c). Scale bar in (A–D):10 μm and in (a–d): 2 μm. Secondary antibodies alone gave no signal (data not shown). (B) Bar graph of the percentage of cells positive to nephrin/PI3K co-localization. Analysis was performed in digital images. In each case, a total of fifty cells from three independent experiments, with imaging of 5–10 cells each, were used to evaluate the number of cells that were positive to nephrin/PI3K co-localization. Data represent the means ± SD; $n = 3$, $^*P < 0.05$ as compared to control cells (cells in the absence of "clustering" antibodies). (For interpretation of the references to color in this figure legend, the reader is referred to the web version of this article.)

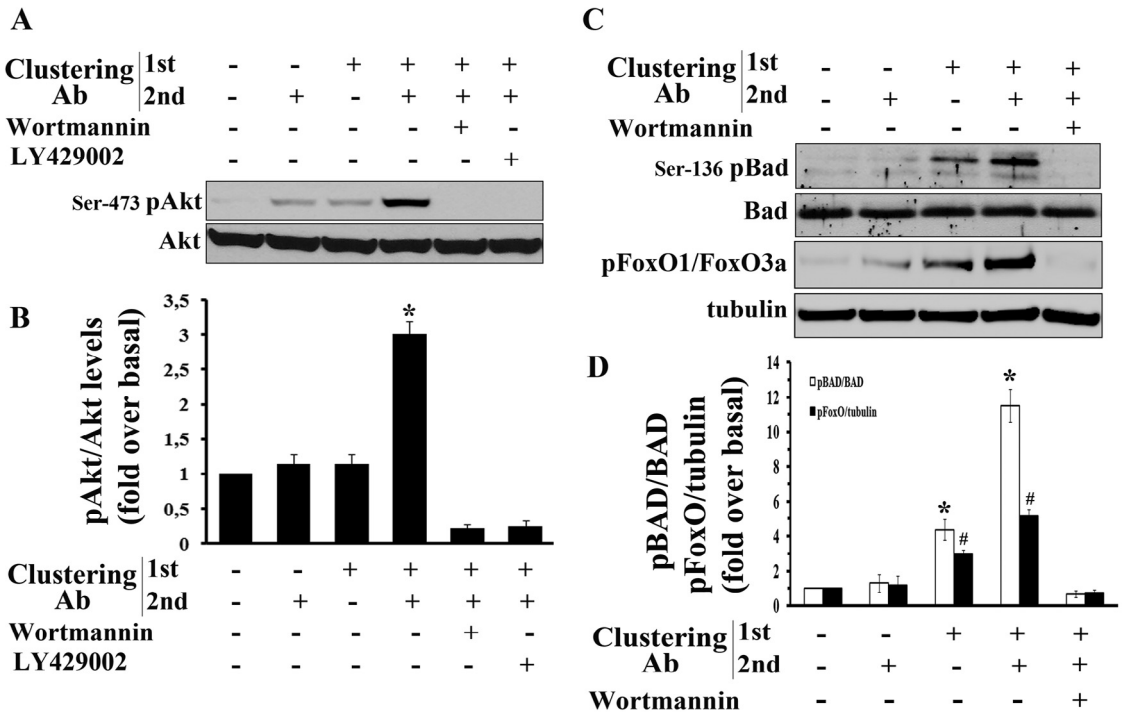

Fig. 4. Nephrin clustering induced PI3K-dependent anti-apoptotic Akt signaling. Cells grown on 24-well plates were incubated or not with "clustering" antibodies, as described in Fig. 2 in the presence or absence of PI3K inhibitors and finally lysed. (A) Representative Western blot of (Ser473) Akt phosphorylation. Immunoblots were stripped and re-probed with anti-Akt antibody to normalize the blots for protein levels. (B) Densitometric quantification of pAkt to Akt levels as fold over basal rate (non-stimulated cells). Data represent the means ± SD; $n = 6$, $^{*}P < 0.05$ as compared to pAkt/Akt levels of non-stimulated cells. (C) Cells grown on 24-well plates were incubated in the presence or absence of "clustering" antibodies and finally lysed; the anti-nephrin antibody (N-20) was added to cells for 30 min on ice and the secondary anti-goat IgG antibody [$F(ab)_2$ fragment] was then added for 30 min at 37 °C. Representative Western blots of (Ser136) Bad and (Thr24) FoxO1/(Thr32) FoxO3a phosphorylation. Immunoblots were stripped and re-probed with anti-Bad or anti-tubulin antibody to normalize the blots for protein levels. (D) Densitometric quantification of pBad to Bad and pFoxO to tubulin levels as fold over basal rate (non-stimulated cells). Data represent the means ± SD; $n = 3$, $^{*}P < 0.05$ as compared to pBad/Bad levels of non-stimulated cells, $^{\#}P < 0.05$ as compared to pFoxO/tubulin levels of non-stimulated cells.

(a selective inhibitor of Src kinases) on nephrin signaling was assessed. We found that 10–20 μM/l^{-1} PP1 completely inhibited clustering-induced phosphorylation of nephrin (Fig. 5A). Pretreatment of cells with 10 μmol/l^{-1} PP1 did not affect clustering of nephrin (Fig. 5B); however, it inhibited both recruitment of PI3K to clustered nephrin (Fig. 5B) and PI3K-dependent signaling in a concentration-dependent manner, as indicated by inhibition of Ser 473 Akt phosphorylation (Fig. 5C,D). These results suggest that Src family kinases mediate nephrin signaling by phosphorylating nephrin on tyrosine residues.

3.5. Targeted suppression of nephrin expression inhibited Akt phosphorylation and increased susceptibility of βTC-6 cell to apoptosis

To establish the role of nephrin in PI3K-Akt signaling, βTC-6 cells were treated or not with 100 nmol/l^{-1} of nephrin-specific siRNA or control (scramble) siRNA, incubated or not with "clustering" antibodies and finally lysed. Western blot analysis of whole cell lysates demonstrated that suppression of nephrin by nephrin-specific siRNA inhibited phosphorylation of Akt induced by "clustering" antibodies (Fig. 6A,B). Transfection of cells with control (scramble) siRNA had no significant effect on nephrin expression and antibody-induced Akt phosphorylation, compared to control cells (cells treated with "clustering" antibodies in the absence of siRNA) (Fig. 6A,B). In nephrin-depleted cells the levels of antibody-induced Akt phosphorylation were similar to those observed in cells incubated in the absence of "clustering" antibodies (Fig. 6A,B). Moreover, no difference was observed in basal Akt phosphorylation of cells transfected with nephrin–siRNA or scramble–siRNA, compared to non-transfected cells (Fig. 6A,B).

In sequence, we investigated the effect of nephrin silencing on cell survival. Beta TC-6 cells were treated or not with nephrin-specific siRNA or control (scramble) siRNA, incubated in the presence or absence of serum for 48 h and finally lysed. Caspase-3 activity was monitored by caspase-processing and cleavage of its downstream target, polyADP ribose polymerase (PARP). The amount of cleaved caspase-3 was previously correlated with pancreatic beta-cell apoptosis (Venieratos et al., 2010); moreover detection of caspase-mediated cleavage of PARP has been established as a hallmark of apoptosis (Luo and Kraus, 2012). Western blotting analysis demonstrated that upon serum withdrawal, βTC-6 cells displayed increased levels of the large fragment (19 kDa) of activated caspase-3 (3.69 ± 0.094) and increased ratio of cleaved/uncleaved PARP (7.49 ± 0.548), compared to cells grown in the presence of serum (1 ± 0.000) (Fig. 6C,D). This effect was further enhanced in nephrin-depleted cells (6.26 ± 0.88 for activated caspase-3 and 13.9 ± 1.01 for PARP cleavage) compared to cells transfected with scramble siRNA (3.84 ± 0.098 for activated caspase-3 and 7.49 ± 0.684 for PARP cleavage) (Fig. 6C,D). In the presence of serum, silencing of nephrin had no effect on basal activation of caspase-3 and PARP cleavage (were not significant in all instances; data not shown). In addition, the degree of apoptosis was evaluated by detection of DNA strand breaks (*in situ* TUNEL and DAPI staining). Analysis of βTC-6 cells for DNA fragmentation (TUNEL-positive cells) revealed that serum deprivation resulted in a sevenfold increase in the number of TUNEL-positive cells, compared to cells grown in the presence of serum (where baseline apoptosis was minimal) (Fig. 6E,F, see also

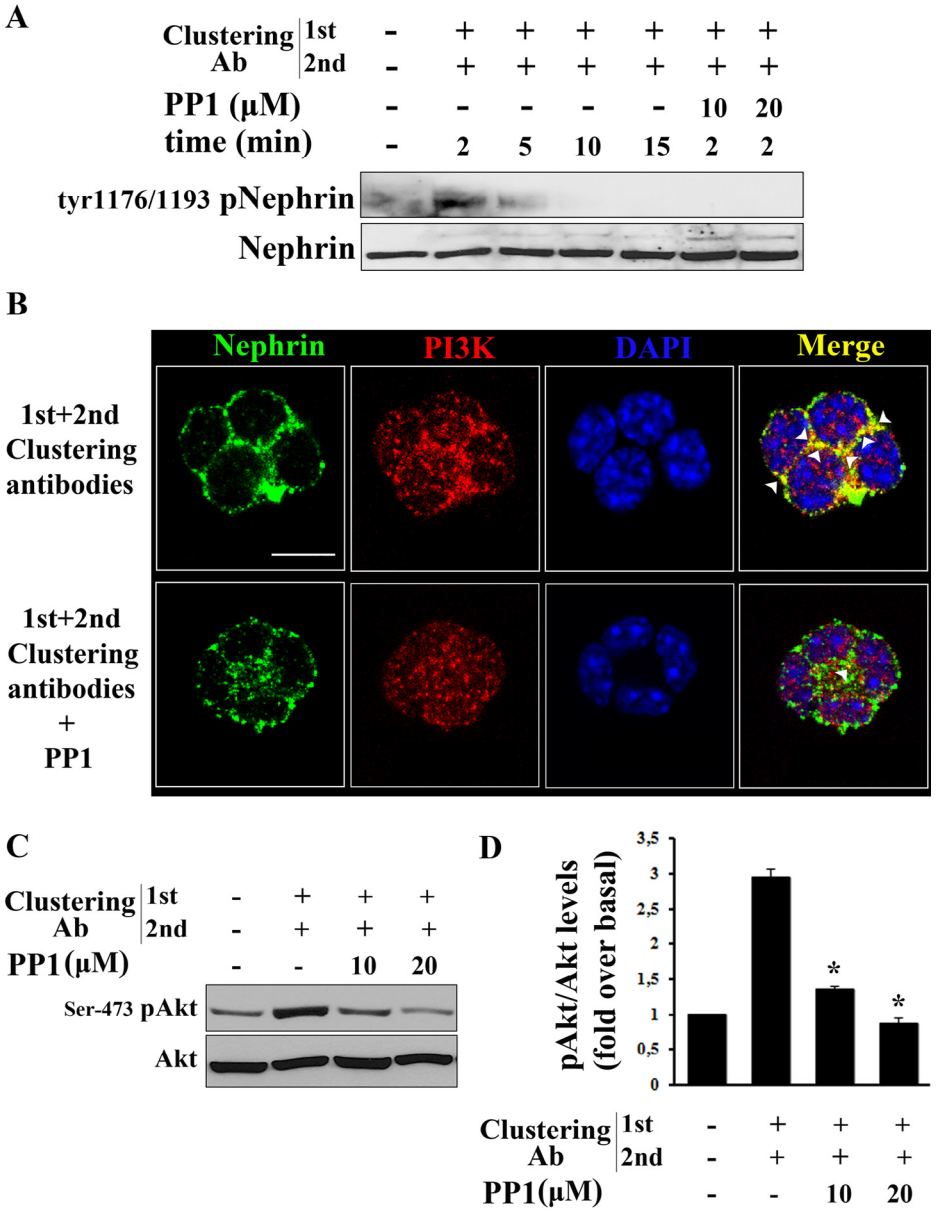

Fig. 5. Nephrin phosphorylation and signaling were inhibited by PP1, a selective inhibitor of Src kinases. (A) Cells grown on 24-well plates were pre-treated or not with 10–20 μmol.l^{-1} PP1 for 1 hour, and then incubated with "clustering" antibodies (anti-nephrin N20: 30 min on ice; secondary antibody IgG [F(ab)$_2$ fragment]: 2–15 min at 37 °C), in the presence or absence of PP1. Cells were lysed and nephrin tyrosine phosphorylation was determined by immunoblotting. The control sample was incubated in the absence of clustering antibodies, both on ice for 30 min and at 37 °C for 15 min. Three independent experiments were performed. Representative Western blot of Tyr 1176/1193 phosphorylation of nephrin. Immunoblots were stripped and re-probed with anti-nephrin antibody to normalize the blots for protein levels. Nephrin clustering induced strong and immediate increase of nephrin phosphorylation on residues Tyr1176/1193, which was inhibited by PP1. (B) Cells grown on glass coverslips were pre-treated or not with 10 μmol.l^{-1} PP1 for 1 hour, and incubated with "clustering" antibodies (anti-nephrin N20: 30 min on ice; secondary antibody IgG [F(ab)$_2$ fragment]: 10–15 min at 37 °C), in the presence or absence of PP1. Cells were then fixed, permeabilized and processed for immunocytochemistry as described in Section 2. Cells were stained with anti-nephrin C17 (recognizes the cytoplasmic tail of nephrin) and anti-p85α^{PI3K} antibodies and the appropriate secondary Alexa-Fuor-antibodies. Nuclei were counterstained with DAPI. Three independent experiments were performed. Representative confocal images of βTC-6 cells stained for nephrin cytoplasmic domain (green) and PI3K (red). Scale bar: 10 μm. In merged images, white arrowheads show regions with nephrin–PI3K co-localization. Secondary antibodies alone gave no signal (data not shown). (C) Cells grown in 24-well plates were pre-treated or not with 10–20 μmol.l^{-1} PP1 for 1 hour. Nephrin was then clustered with "clustering" antibodies (as described in Fig. 5B), in the presence or absence of PP1. Cells were lysed and Akt phosphorylation was assessed by immunoblotting. Representative Western blot of (Ser-473) Akt phosphorylation. Immunoblots were stripped and re-probed with anti-Akt antibody to normalize the blots for protein levels. (D) Densitometric quantification of pAkt to Akt levels as fold over basal rate (non stimulated cells). Data represent the means ± SD; $n = 3$, $^*P < 0.05$ as compared to pAkt/Akt levels of stimulated cells in the absence of PP1 inhibitor. (For interpretation of the references to color in this figure legend, the reader is referred to the web version of this article.)

Supplementary file 3). Susceptibility to apoptosis was further enhanced in nephrin-depleted cells (27.43 ± 3.01) compared to cells transfected with control (scramble) siRNA (13.76 ± 1.48) (Fig. 6E,F, see also Supplementary file 3). Taken together the earlier results confirmed the pivotal involvement of nephrin in PI3K-mediated Akt signaling and cell survival.

3.6. High glucose impaired nephrin signaling

We next studied the effects of high glucose concentration on nephrin tyrosine phosphorylation and Ser473 Akt phosphorylation in βTC-6 cells. Cells grown in the presence of 1 mmol.l^{-1} glucose were exposed to 25 mmol.l^{-1} glucose for 48 hours, and then stimulated with

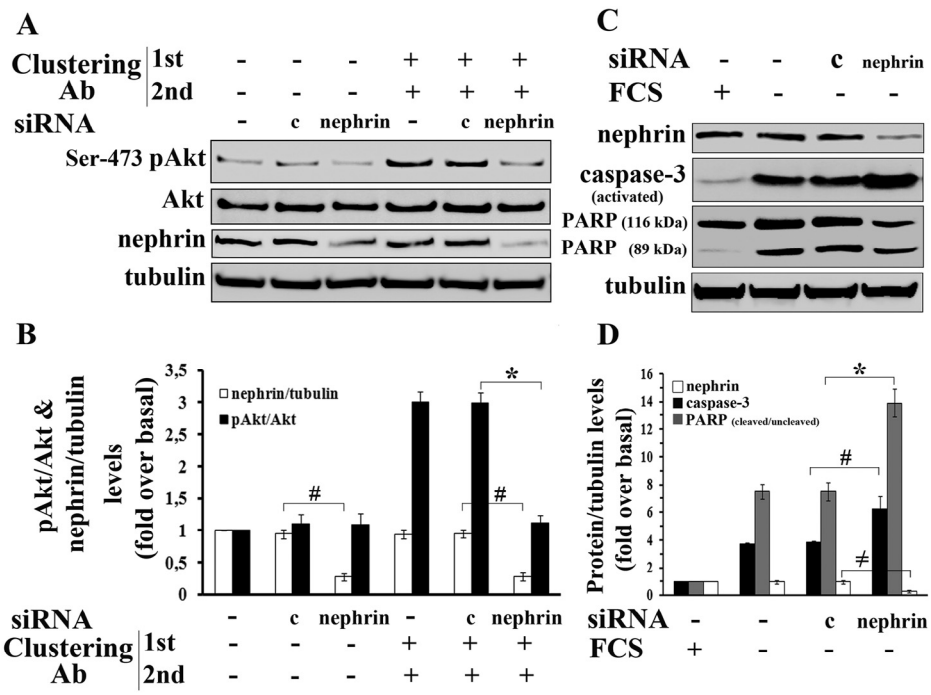

Fig. 6. Silencing of nephrin inhibited nephrin-induced Akt phosphorylation and increased susceptibility of βTC-6 cells to apoptosis. Beta TC-6 cells grown in the presence of 1 mmol.l^{-1} glucose were transfected with either control (scramble) siRNA or nephrin-specific siRNA as described in Section 2. At the end of the incubation period, cells were treated or not with "clustering" antibodies as described in Fig. 2, lysed and nephrin suppression and (Ser 473) Akt phosphorylation were evaluated by immunoblotting. (A) Representative Western blots of pAkt and nephrin. Immunoblots were stripped and re-probed with anti-Akt or anti-tubulin antibody to normalize the blots for protein levels. (B) Densitometric quantification of pAkt to Akt and nephrin to tubulin levels as fold over basal rate (non-transfected, non stimulated cells). Data represent the means ± SD; $n = 3$, $^{*}P < 0.05$ as compared to pAkt/Akt levels of stimulated cells treated with control siRNA and $^{\#}P < 0.05$ as compared to nephrin/tubulin levels of cells treated with control siRNA. (C) Nephrin-depleted and control βTC-6 cells were incubated for 48 hours in the absence of serum. Cell apoptosis was evaluated by detection of caspase-3 activation and PARP cleavage. Representative Western blots of cleaved (activated) caspase-3 and PARP cleavage pattern. Immunoblots were stripped and re-probed with anti-tubulin antibody to normalize the blots for protein levels. (D) Densitometric quantification of activated caspase-3 and cleaved/uncleaved PARP to tubulin levels as fold over basal rate of activated caspase-3 and PARP (cells grown in the presence of serum). Data represent the means ± SD; $n = 3$, $^{\#}P < 0.05$ as compared to activated caspase-3/tubulin levels of cells treated with control siRNA, $^{*}P < 0.05$ as compared to cleaved/uncleaved PARP/tubulin levels of cells treated with control siRNA, $^{\neq}P < 0.05$ as compared to nephrin/tubulin levels of cells treated with control siRNA. (E) Nephrin-depleted and control βTC-6 cells were incubated for 48 hours in the absence of serum. Cell apoptosis was evaluated by *in situ* TUNEL and DAPI staining. Representative confocal images of apoptotic cells (red: *in situ* TUNEL; blue: DAPI). Magnification: ×400. Cells treated with 200 nmol.l^{-1} of staurosporine for 18 hours, served as positive control for induction of apoptosis, whereas cells incubated with labeling reaction mixture in the absence of TdT enzyme or cells growing in the presence of serum served as negative control. (F) Quantification of the percentage of cells undergoing apoptosis. In each case, a total of 1000–1500 cells from three independent experiments were used to evaluate the number of TUNEL-positive cells. Data represent the means ± SD; $n = 3$, $^{*}P < 0.05$ as compared to cells treated with control siRNA. (For interpretation of the references to color in this figure legend, the reader is referred to the web version of this article.)

"clustering" antibodies (anti-nephrin N20: 30 min on ice; secondary antibody IgG [F(ab)$_2$ fragment]: 2 min at 37 °C, for nephrin phosphorylation experiments or 15 min at 37 °C, for Akt phosphorylation experiments). In the presence of "clustering" antibodies, Tyr 1176/1193 nephrin phosphorylation was significantly impaired in cells exposed for 48 hours to 25 mmol.l^{-1} glucose (0.66 ± 0.051) compared to the control (3.71 ± 0.355) (cells growing in 1 mmol.l^{-1} glucose) (Fig. 7). Similarly, Ser473 Akt phosphorylation was significantly reduced in cells exposed for 48 hours to 25 mmol.l^{-1} glucose (1.41 ± 0.065) compared to the control (3.12 ± 0.177) (cells growing in 1 mmol.l^{-1} glucose) (Fig. 7). Notably, the addition of the primary N20 antibody alone, without a secondary clustering antibody, also induced nephrin phosphorylation in control cells (cells growing in 1 mmol.l^{-1} glucose), but the induction was considerably lower compared to that observed in the presence of both "clustering" antibodies (Fig. 7). High glucose concentration had no significant effect on nephrin expression in β-TC6 cells (densitometric quantification not shown).

3.7. High glucose increased nephrin internalization and PKCα expression

The effect of glucose concentration on sub-cellular localization of nephrin was examined in βTC-6 cells. Cells growing on glass coverslips were exposed to 25 mmol.l^{-1} glucose for 48 hours, fixed, permeabilized, and stained with anti-nephrin C17 antibody. Confocal microscopy revealed that nephrin was primarily localized within numerous small clusters at the plasma membrane as well as at sites of cell contact, in cells cultured in 1 mmol.l^{-1} glucose (Fig. 8A). Exposure of cells to 25 mmol.l^{-1} glucose resulted in merging of nephrin clusters to larger, numerous intracellular vesicles, suggesting increased internalization of nephrin (Fig. 8A). Decreased availability of cell surface-associated nephrin could help explain the observed impairment of nephrin induced-Akt phosphorylation (Fig. 7). Since PKCα-dependent nephrin internalization (endocytosis) was reported to occur in podocytes, as a result of hyperglycemia (Quack et al., 2006, 2011), the expression of PKCα was examined. Western blot analysis demonstrated markedly increased PKCα protein expression in cells exposed to 25 mmol.l^{-1} glucose for 24 h (1.68 ± 0.080) or 48 h (2.55 ± 0.111) compared to cells growing in 1 mmol.l^{-1} glucose (1 ± 0.000) (white bar) (Fig. 8B,C). Taken together the earlier results suggest that up-regulation of PKCα expression might be involved in glucose-induced nephrin internalization.

3.8. Nephrin expression and Akt phosphorylation were reduced in diabetic (db/db lepr−/−) mouse model

To investigate the effect of chronic hyperglycemia on nephrin expression and signaling, we performed *in vivo* studies in the animal model of C57BL/KsJ *db/db* mice. These mice express defective leptin

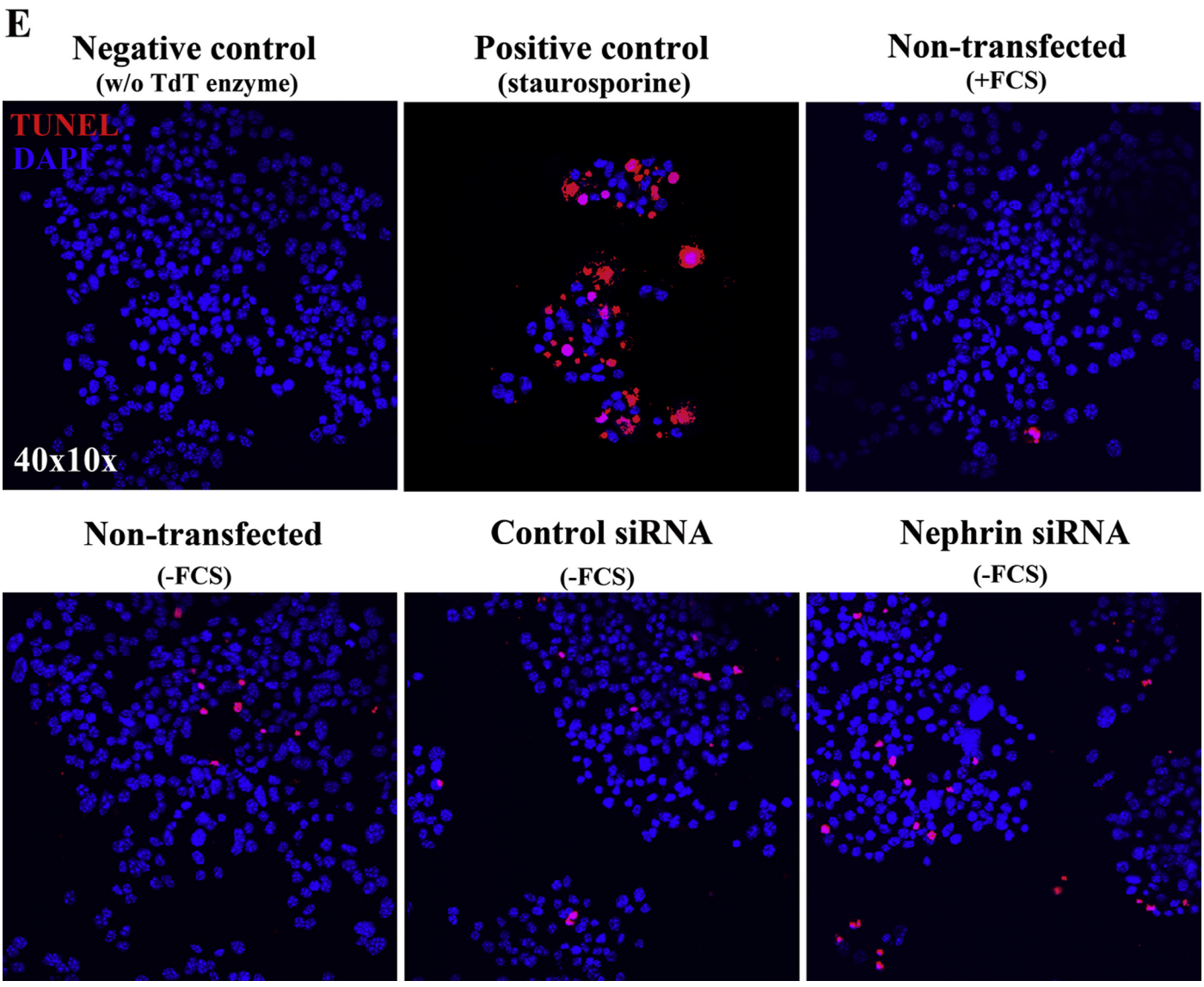

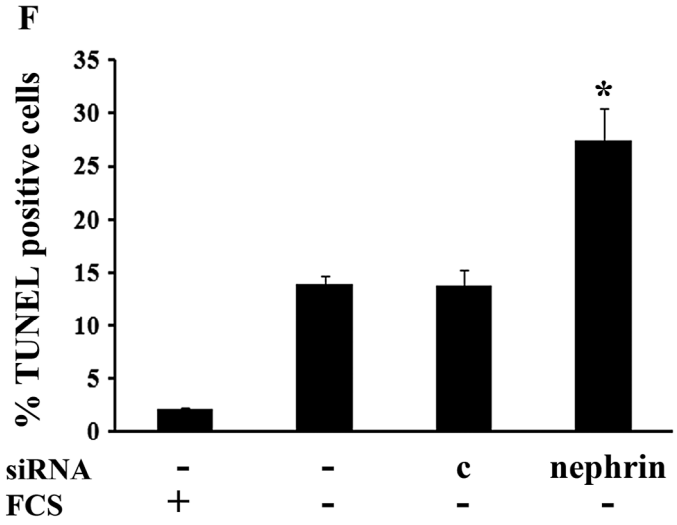

Fig. 6. (*continued*)

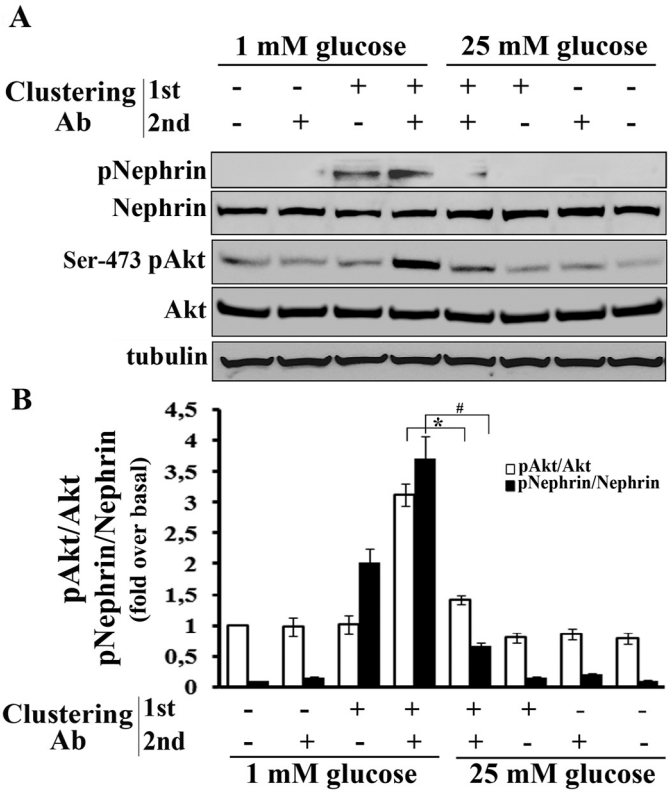

Fig. 7. High glucose impaired nephrin signaling. Beta TC-6 cells continuously grown in DMEM containing 1 mmol.l^{-1} glucose were exposed for 48 hours to 25 mmol.l^{-1} glucose, incubated or not with "clustering" antibodies (anti-nephrin N20: 30 min on ice; secondary antibody IgG [F(ab)$_2$ fragment]: 2 min at 37 °C, for nephrin phosphorylation experiments or 15 min at 37 °C, for Akt phosphorylation experiments) and finally lysed. (A) Representative Western blots of tyr 1176/1193 nephrin phosphorylation and Ser 473 Akt phosphorylation. Immunoblots were stripped and reprobed with anti-nephrin, anti-Akt or anti-tubulin antibodies to normalize the blots for protein levels. (B) Densitometric quantification of pNephrin to Nephrin and pAkt to Akt levels as fold over basal rate (non-stimulated cells in 1 mmol.l^{-1} glucose). Data represent the means ± SD; $n = 3$, $^{\#}P < 0.05$ as compared to pNephrin/Nephrin levels of stimulated cells in 1 mmol.l^{-1} glucose, $^{*}P < 0.05$ as compared to pAkt/Akt levels of stimulated cells in 1 mmol.l^{-1} glucose. Densitometric quantification of nephrin to tubulin levels (data not shown) revealed no significant changes in nephrin expression between cells grown in 1 mmol.l^{-1} glucose and cells grown in 25 mmol.l^{-1} glucose.

receptor and are a well-established model of type 2 diabetes, since they are obese and hyperinsulinemic and exhibit pronounced hyperglycemia after the 8th wk of age (Chen et al., 1996; Diani et al., 2004). Five animals (*db/db* lepr–/–) and five animals (db/db lepr +/–) were used as experimental diabetic model and control respectively. Mice were euthanized at the 10th wk after birth. Dual fluorescence immunohistochemical studies with nephrin and insulin or Ser473-pAkt and insulin, in mouse pancreatic sections, revealed that the islets of lepr–/– diabetic animals exhibited a significant decrease in the levels of nephrin/per unit of islet area (44.7 ± 4.80) compared with islets of lepr+/– animals used as control (80.35 ± 14.02) (Fig. 9A,C). Interestingly, intense nephrin staining was also detected in the exocrine pancreas of db/db lepr+/– mice and moreover exocrine pancreatic nephrin appeared to be decreased in diabetic animals (Fig. 9A). Pre-incubation of anti-nephrin N20 antibody with its specific blocking peptide was found to significantly reduce immune-reactivity, thus confirming the specificity of the antibody (Fig. 9A, negative control 2). Staining of mouse pancreata sections with insulin (red) and the secondary antibody anti-goat IgG-Alexa Fluor 488 (green) alone gave no signal for nephrin (Fig. 9A, negative control 1). Furthermore, the islets of diabetic animals exhibited a considerable decrease in the levels of phosphorylated Akt/per unit of islet area (49.43 ± 11.90), compared with islets of control animals (109.33 ± 11.74) (Fig. 9B,C). Differences in nephrin and pAkt fluorescence intensity between the two islet populations were statistically significant ($P < 0.05$) (Fig. 9C). These results indicate that the reduction of both nephrin and phosphorylated Akt in islet β-cells may be a consistent feature of type 2 diabetes.

4. Discussion

Nephrin is a cell surface receptor participating in cell–cell adhesion and signaling functions in glomerular podocytes (Welsh and Saleem, 2010). Recent studies supported a primary role of nephrin as regulator of actin cytoskeleton remodeling in pancreatic beta-cells, similar to what has been described in podocytes (Fornoni et al., 2010; Jeon et al., 2012).

The present study focused on the role of nephrin as signal transducing receptor in pancreatic beta-cells. We utilized endogenous nephrin expression in cultured pancreatic βTC-6 cells to establish a role for nephrin in pancreatic beta-cell survival signaling. We demonstrated that pancreatic beta-cell nephrin interacted/associated with the p85α regulatory subunit of PI3K *in situ* in mouse islet β-cells and in cultured βTC-6 cells. Similar interactions were reported to regulate renal podocyte morphology and function (Benzing, 2004). Nephrin signaling can be experimentally induced by anti-nephrin antibodies (Lahdenpera et al., 2003), over-expression of podocin and the Src kinase Fyn (Li et al., 2004; Liu et al., 2004; Verma et al., 2003, 2006), nephrin interaction with Neph1 (Garg et al., 2007), or nephrin homophilic interactions (Barletta et al., 2003). To further document interactions between nephrin and PI3K we used functional, specific anti-nephrin antibodies against an extracellular domain of this protein, to assess the effects of nephrin–ligand binding on nephrin signaling. In this instance, clustering of nephrin on the plasma membrane by antibodies, induced phosphorylation of 1176/1193 tyrosine residues of nephrin and recruited PI3K to clustered nephrin. PI3K recruitment resulted in activation of PI3K, since it was associated with activation of Akt. Clustering-induced signaling events were inhibited by PP1, indicating that Src family kinases mediate nephrin signaling by phosphorylating nephrin on tyrosine residues. It has been reported that in renal cells, clustering of nephrin induced phosphorylation of several tyrosine residues, including tyrosines 1176 and 1193, of the cytoplasmic domain of nephrin by Src kinases *in vivo* and *in vitro*, thus augmenting and/or facilitating the engagement of several SH2–SH3 domain-containing signaling molecules (Huber et al., 2003a; Jones et al., 2006; Lahdenpera et al., 2003; Li et al., 2004; New et al., 2013; Verma et al., 2003, 2006). Phosphorylation of 1176/1193 tyrosine residues of nephrin also play a role in glucose-stimulated insulin release (GSIR) by pancreatic beta cells (Jeon et al., 2012). In podocytes, following phosphorylation, the intracellular domain of nephrin interacted with several proteins, including Neph1, podocin, CD2AP, PI3K, Nck, β-arrestin-2, PKCα and PLCγ1. These interactions transmit nephrin signaling to the actin cytoskeleton and regulate survival, endocytosis and metabolism (Harita et al., 2009; Huber et al., 2001, 2003a; Lehtonen et al., 2002; Quack et al., 2011; Shih et al., 2001; Tossidou et al., 2010).

CD2AP has been detected in pancreatic extracts (Rinta-Valkama et al., 2007), however its localization was not defined. Our results documented that both islet β-cells and βTC-6 cells express CD2AP which is also associated with nephrin. CD2AP was reported to interact with both nephrin and PI3K *in vivo*, stimulating anti-apoptotic Akt signaling in podocytes (Huber et al., 2003a). It is possible then that CD2AP also potentiates nephrin signaling in pancreatic beta-cells. Interestingly, we found that nephrin and CD2AP were also expressed by exocrine pancreatic tissue (acinar cells) and moreover co-localized, although nephrin expression has been reported to occur exclusively in the β-cells (Palmen et al., 2001; Rinta-Valkama

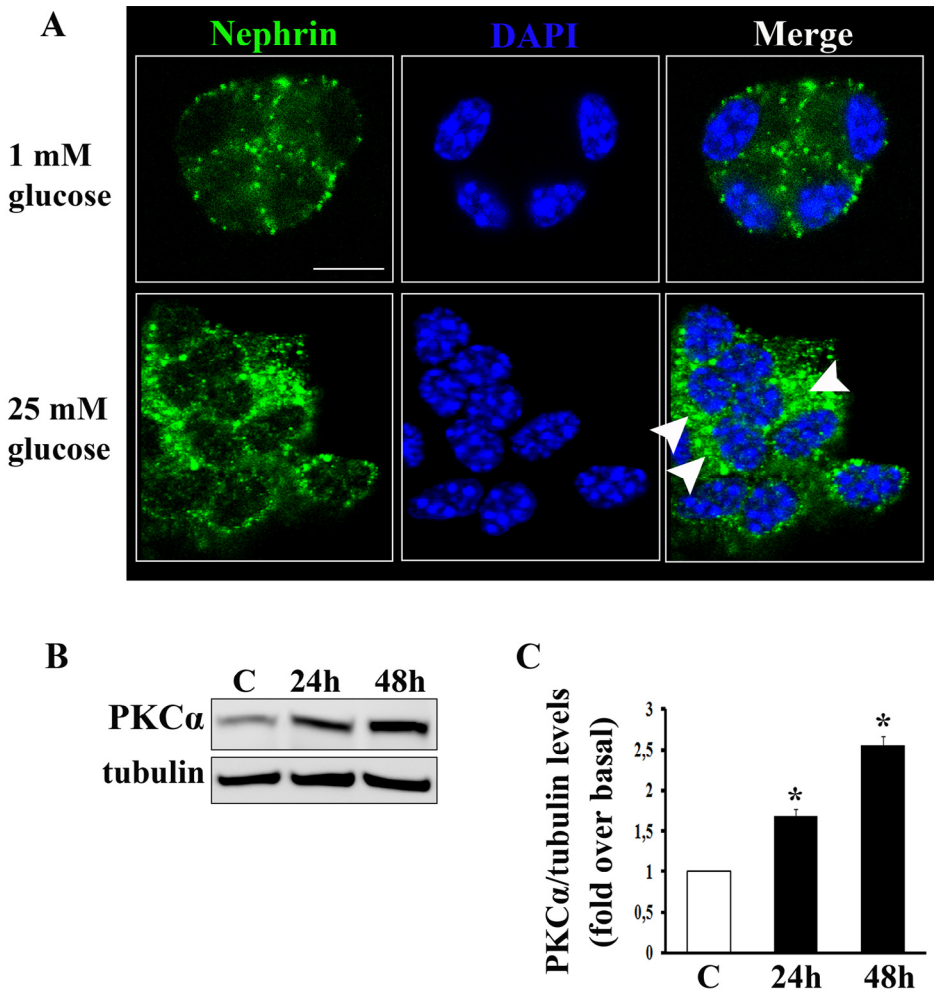

Fig. 8. High glucose induced nephrin internalization and up-regulated PKCα expression. (A) Beta TC-6 cells grown on glass coverslips in DMEM containing 1 mmol.l^{-1} glucose were exposed for 48 hours to 25 mmol.l^{-1} glucose, fixed, permeabilized and stained with anti-nephrin C17 antibody (recognizes the cytoplasmic tail of nephrin) and the appropriate secondary Alexa-Fluor-antibody. Nuclei were counterstained with DAPI. Three independent experiments were performed. Representative confocal images of βTC-6 cells stained for nephrin cytoplasmic domain (green). In 1 mmol.l^{-1} glucose, nephrin is predominantly localized to the plasma membrane and at the sites of cell–cell contact. Upon exposure to 25 mmol.l^{-1} glucose, nephrin undergoes, in part, internalization (white arrowheads show regions where nephrin localized in numerous intracellular vesicles). Scale bar: 10 μm. Secondary antibody alone gave no signal (data not shown). (B) Beta TC-6 cells continuously grown in DMEM containing 1 mmol.l^{-1} glucose were exposed for 24 or 48 hours to 25 mmol.l^{-1} glucose and finally lysed. Representative Western blot of PKCα expression. Immunoblots were stripped and re-probed with anti-tubulin antibody to normalize the blots for protein levels. (C) Densitometric quantification of PKCα to tubulin levels as fold over basal rate (cells growing in the presence of 1 mmol.l^{-1} glucose; white bar). Data represent the means ± SD; $n = 3$, $^{*}P < 0.05$ as compared to PKCα/tubulin levels of cells in 1 mmol.l^{-1} glucose (white bar). (For interpretation of the references to color in this figure legend, the reader is referred to the web version of this article.)

et al., 2007). This discrepancy may be attributed to differences in the antigenic-epitope targeted by the antibodies, differences in the suitability of antibodies used in various applications together with differences in tissue collection protocols. Although the role of nephrin in pancreatic exocrine tissue remains to be established, it is likely that in acinar cells, nephrin is involved in the structural machinery that forms secretory granules leading to secretion of digestive enzymes by exocytosis, a role consistent to that has been described in β-cells (Fornoni et al., 2010).

Akt provides a strong survival signal that protects cells from death induced by various stresses (Datta et al., 1999). According to our results, nephrin–PI3K-induced Akt activation was accompanied by phosphorylation, hence inhibition, of pro-apoptotic Bad protein and suppression of FoxO1/3a transcription factors. In addition, silencing of nephrin expression resulted in impairment of nephrin-mediated Akt activation accompanied by increased susceptibility of cells to environmental stress. In cultured podocytes, nephrin-induced activation of PI3K and its downstream target Akt was associated with strong inhibition of detachment induced-apoptosis (anoikis) (Huber et al., 2003a). Moreover, the importance of unperturbed Akt signaling for beta-cell survival was also documented by our previous work, in which high glucose attenuated insulin-induced Akt activation and enhanced susceptibility of beta-cells to apoptosis (Venieratos et al., 2010). Our current results substantiated a pivotal role for nephrin in pancreatic beta-cell survival, through nephrin-induced PI3K/Akt anti-apoptotic signaling and highlight the importance of tyrosine phosphorylation of nephrin for nephrin–PI3K interaction and Akt activation.

The significance of nephrin signaling *in vivo* was previously well documented in glomerular podocytes. Several studies confirmed that nephrin molecules from adjacent foot processes bind to each other. In addition, Neph1 was shown to serve as a binding partner of the extracellular domain of nephrin. These data suggested that *cis* and *trans* interactions involving at least nephrin and Neph1 Ig superfamily proteins are required for setting up an intact slit diaphragm structure and induce efficient nephrin signal transduction (Barletta et al., 2003; Gerke et al., 2003; Khoshnoodi et al., 2003). *In vivo*, beta-cells are aggregated in the form of islets in the pancreas, where they

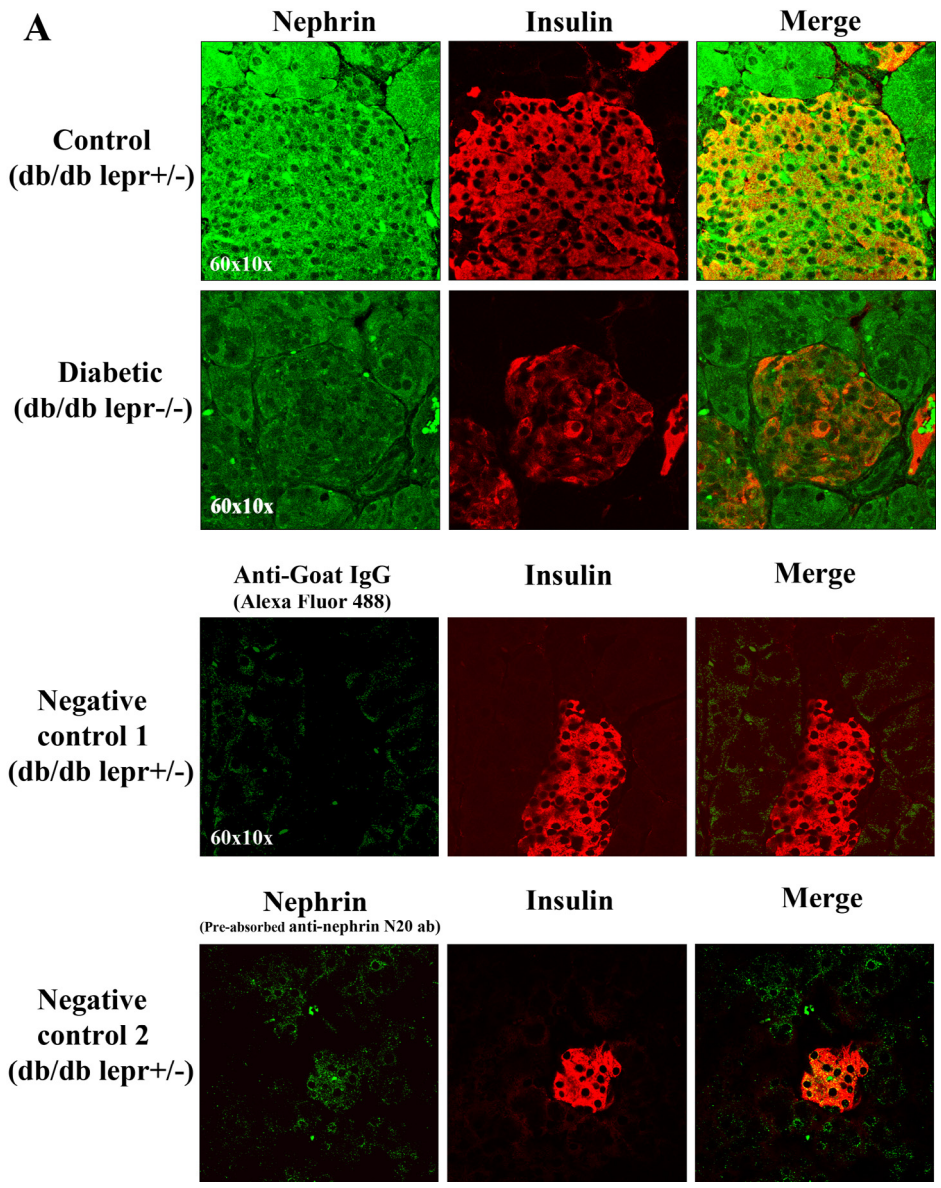

Fig. 9. Nephrin expression and pAkt levels are reduced in diabetic (*db/db* lepr–/–) mouse model. Nephrin and insulin or Ser 473 pAkt and insulin were detected by fluorescence immunohistochemistry in sections of formalin-fixed paraffin-embedded murine pancreata from C57BL/KsJ *db/db* mice with a defective leptin receptor (lepr–/–). Five animals were used as experimental diabetic model (*db/db* lepr–/–), and five animals were used as control (db/db lepr+/–). Mice were euthanized at the 10th wk after birth. (A) Representative confocal images of mouse pancreas sections from (lepr–/–) animal show reduced expression of nephrin (green) in the pancreatic islet stained for insulin (red) compared with the pancreatic islet of control (lepr+/–) animal. Magnification: ×600. Staining of mouse pancreata sections with insulin (red) and the secondary antibody anti-goat IgG-Alexa Fluor 488 (green) alone gave no signal for nephrin (negative control 1). In pre-absorption experiments, the anti-nephrin N20 antibody (0.2 mg/ml) was pre-incubated with its specific blocking peptide [nephrin (N20) P, sc-1990P, 0.2 mg/ml)] at 1:2 ratio, overnight at 4 °C and the mixture was used for immunofluorescent detection of nephrin. The results showed a significant decrease of fluorescence intensity (negative control 2) in comparison to the immunostaining using anti-nephrin antibody that was not pre-incubated with its specific blocking peptide. (B) Representative confocal images of mouse pancreas sections from (lepr–/–) animal show reduced levels of phosphorylated Akt (red) in the pancreatic islet stained for insulin (green) compared with the pancreatic islet of control (lepr+/–) animal. Magnification: ×600. Staining of mouse pancreata sections with insulin (green) and the secondary antibody anti-rabbit IgG-Alexa Fluor 594 (red) alone gave no signal for pAkt (negative control). Dual immunofluorescence in specimens was viewed with a BIORAD confocal laser-scanning microscope. (C) Quantification of islet nephrin and pAkt levels (nephrin or pAkt fluorescence intensity/unit of islet area). Data represent the means ± SD from measurements of 20–30 independent islets per group (4–6 islets per mouse pancreas were randomly chosen from five animals per group). Differences in nephrin or pAkt fluorescence intensity/unit of islet area between the two islet populations were found statistically significant (one-way ANOVA and Mann–Whitney non parametric test, $^{*}P < 0.05$ as compared to nephrin expression in control islets, $^{\#}P < 0.05$ as compared to pAkt levels in control islets). (For interpretation of the references to color in this figure legend, the reader is referred to the web version of this article.)

communicate with each other. Communication between β-cells has been known to modulate insulin secretion, via receptor tyrosine kinases of the Eph family which bind to cell surface-associated ephrin ligands on neighboring cells. The ensuing bidirectional signals have emerged as a major form of contact-dependent intercellular communication (Konstantinova et al., 2007). Accordingly, it appears likely that nephrin homo- and/or heterophilic interactions occur in pancreatic islet beta-cells as a consequence of cell–cell contact within the islets, resulting in signaling events which apparently regulate and promote cell survival.

A great variety of nephrin gene mutations has been described, including insertions, deletions, nonsense and missense mutations, which are responsible for congenital nephrotic syndrome (CNS) of the Finnish type (Kestila et al., 1998; Lenkkeri et al., 1999). These

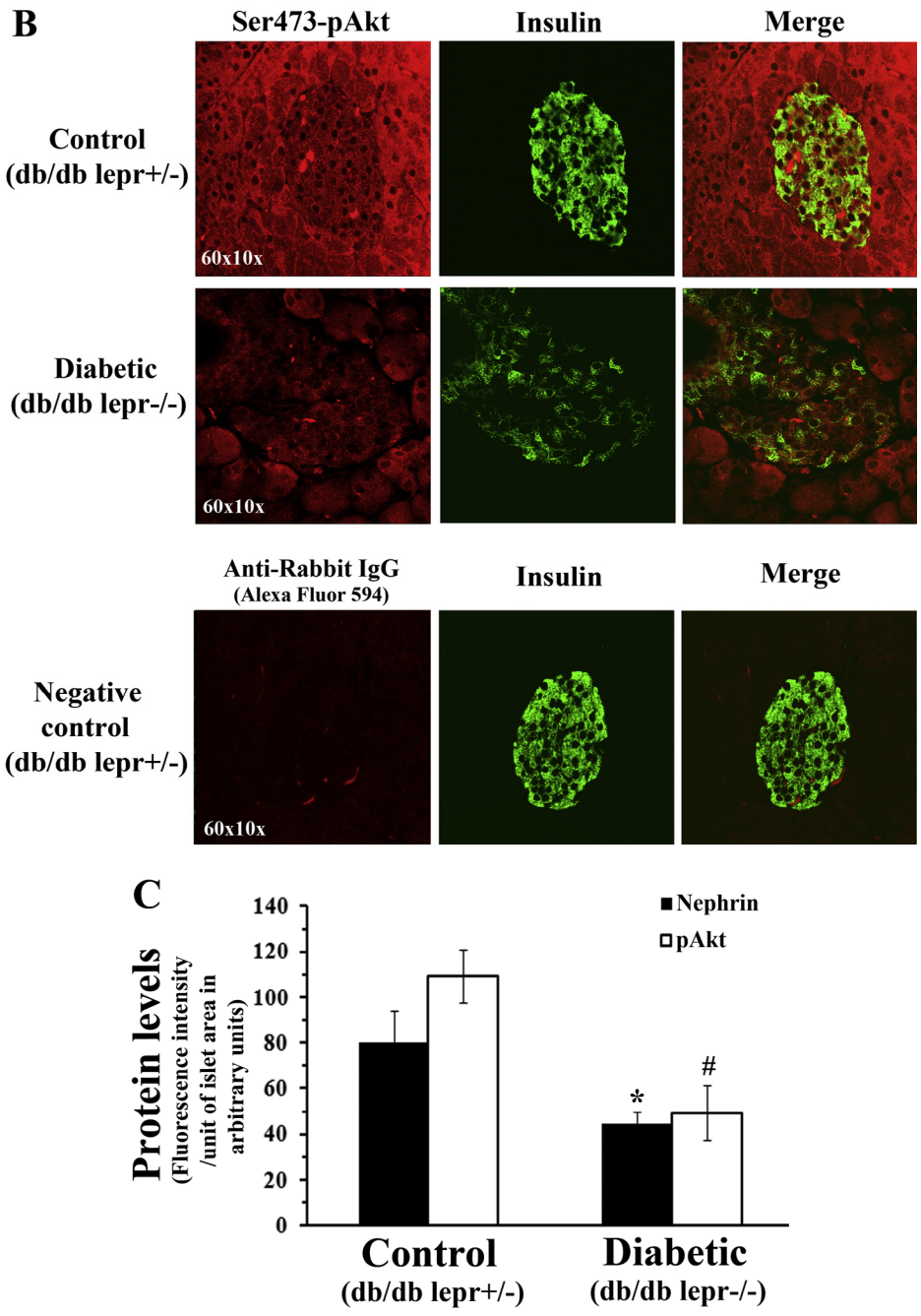

Fig. 9. (*continued*)

mutations lead to severe or to a less severe clinical presentation of CNS. However, patients with CNS neither develop diabetes nor have major defects in other organs than the kidney; minor neurological problems during the nephrotic stage have been observed which were improved after renal transplantation (Patrakka et al., 2000). Apart from obvious species differences, the lack of symptoms in the majority of human subjects with CNS could have several explanations. It is possible that, when nephrin is totally absent or defective, other beta-cell survival signaling pathways prevail (before and after renal transplantation), including the insulin-dependent insulin receptor-IRS2-PI3K-Akt pathway (Venieratos et al., 2010). The same likely occurs in the heart, where nephrin plays a role in vessel formation (Wagner et al., 2011) or in the central nervous system (CNS) where nephrin recruits synaptic vesicles and clusters glutamate receptors linking them to downstream signaling proteins; nephrin alterations in the CNS can be rescued by other Ig-like cell adhesion molecules (Ig-like CAMs) (Li et al., 2011). In fact, it is not rare the role of a mutated protein to be rescued and performed by other proteins in different tissues, generating diverse tissue specific phenotypes.

Chronic hyperglycemia disrupts signal transduction pathways involved in beta-cell survival, leading to the destruction of endocrine pancreas in type 2 diabetes (Cnop et al., 2005). Doublier et al. (2003) demonstrated a decrease of glomerular nephrin expression as an early event in diabetes. Decreased nephrin expression was also reported in islets from several patients with type 2 diabetes (Fornoni et al., 2010). We demonstrated herein that short-term exposure of cultured βTC-6 cells to high glucose impaired clustering-induced

nephrin phosphorylation and Akt activation without affecting nephrin expression. Our immunohistochemical studies in pancreatic islets of type 2 diabetic *(db/db lepr–/–)* mice revealed an *in vivo* reduction of nephrin expression which was accompanied by significantly decreased levels of phosphorylated Akt. However, impairment of Akt phosphorylation could also be attributed, at least in part, to defective insulin signaling within beta-cells, since both insulin secretion/action and expression of multiple insulin signaling proteins are reduced in islets of mice and patients with type 2 diabetes (Goldfine and Kulkarni, 2012). Therefore, decreased nephrin expression and signaling in islet beta-cells may contribute to the pathogenesis of type 2 diabetes.

An additional finding of the present study was the observed reduced nephrin expression in acinar cells of *(db/db lepr–/–)* diabetic mice. There is increasing evidence that both pancreas morphology and exocrine pancreatic function are very frequently severely altered in patients with diabetes mellitus (Hardt and Ewald, 2011). Thus, reduced nephrin expression in acinar cells of diabetic mice might contribute to pancreatic exocrine insufficiency which is increased during the progression of diabetes mellitus.

Recent evidence indicated that hyperglycemia led to up-regulation of PKCα expression in murine podocytes, glomeruli, and kidneys resulting in PKCα-mediated, β-arrestin-2-dependent endocytosis of nephrin (Quack et al., 2011; Tossidou et al., 2010). Our data indicated that in cultured βTC6 cells, high glucose led to increased expression of PKCα accompanied by enhanced nephrin internalization and suggest that glucose-induced impairment of nephrin-mediated Akt signaling could be partly explained by decreased availability of beta-cell surface nephrin. It is possible that nephrin internalization serves as an ignition spark for impaired beta-cell signaling in long-standing hyperglycemia. Moreover, phosphorylation-dependent nephrin trafficking (endocytosis) is also essential for promoting glucose-stimulated insulin response (GSIR) and facilitating proper secretory vesicle formation and exocytosis in pancreatic beta-cells (Fornoni et al., 2010; Jeon et al., 2012). Nephrin internalization could also result in receptor desensitization, further documenting its role as cell surface signal transducer (Quack et al., 2006). Although additional studies are needed to further confirm glucose-induced nephrin internalization, nephrin trafficking seems to be an important mechanism involved in both physiological and pathological conditions.

In summary, the work described herein unraveled a pivotal role for nephrin in pancreatic beta-cell survival signaling, pointing to an anti-apoptotic function not limited to renal cells. A model system is proposed, in which nephrin clustering on the cell surface, via nephrin–nephrin interactions, results in nephrin phosphorylation, recruitment and activation of PI3K, which in turn triggers Akt activation. Akt promotes cell survival by inhibiting apoptosis through phosphorylation and inactivation of pro-apoptotic targets including Bad and FoxO. Short-term exposure of beta-cells to high glucose increases nephrin internalization, possibly in a PKCα-dependent manner, leading to impairment of pancreatic beta-cell nephrin mediated-Akt survival signaling. Gradual reduction of nephrin expression accompanied by decreased Akt activity in long-standing hyperglycemia may further affect islet beta-cell survival. Our data suggest an additional mechanism which may contribute to gradual pancreatic beta-cell loss occurring in type 2 diabetes. Further understanding of the mechanism(s) of islet beta-cell degeneration at the molecular level will contribute to the development of novel drug/therapeutic targets for the treatment of type 2 diabetes.

Note

A patent application, with the title "Pharmaceutical compound containing the N20 antibody, which recognizes nephrin, for the treatment of type 2 diabetes" (*Number: 20130100425/19-07-2013, E. Tsilibary and P. Kitsiou*), has been submitted to Hellenic Industrial Property Organization.

Acknowledgements

This work was supported by the General Secretariat of Research and Technology, Ministry of Education and Religious Affairs through the Operational Programme "Education and Lifelong Learning, ESPA 2007–2013" (Action: "Excellence", Title: "Common pathogenetic pathways and mechanisms of cell apoptosis in Alzheimer and Diabetes disease" DIABET-AL 164); (Action: "Collaboration 2011", Title: "Pancreatic beta cells functionality and regeneration: the role of liraglutide" 11ΣΥΝ_1_1496); (Action: "KRHPIS", Title: "Identification of targets for diagnosis and treatment of diseases" DIAS OPS 448325). The funding sources had no involvement in study design, in the collection, analysis and interpretation of data, in the preparation and writing of the article and also in the decision to submit the paper for publication. The authors wish to thank Eleni Kotsopoulou, M.Sc. (Institute of Biosciences & Applications, N.C.S.R. "Demokritos") for expert technical assistance and Dr. Marina Sagnou and Lefteris Tsalavoutas-Psarras, M.Sc. (Institute of Biosciences & Applications, N.C.S.R. "Demokritos") for expert assistance in confocal microscopy of pancreatic sections.

Appendix: Supplementary Material

Supplementary data to this article can be found online at doi:10.1016/j.mce.2014.11.003.

References

Aoyama, T., Kamata, K., Yamanaka, N., Takeuchi, Y., Higashihara, M., Kato, S., 2006. Characteristics of polyclonal anti-human nephrin antibodies induced by genetic immunization using nephrin cDNA. Nephrol. Dial. Transplant. 21, 1073–1081.
Barletta, G.M., Kovari, I.A., Verma, R.K., Kerjaschki, D., Holzman, L.B., 2003. Nephrin and Neph1 co-localize at the podocyte foot process intercellular junction and form cis hetero-oligomers. J. Biol. Chem. 278, 19266–19271.
Benzing, T., 2004. Signaling at the slit diaphragm. J. Am. Soc. Nephrol. 15, 1382–1391.
Boute, N., Gribouval, O., Roselli, S., Benessy, F., Lee, H., Fuchshuber, A., et al., 2000. NPHS2, encoding the glomerular protein podocin, is mutated in autosomal recessive steroid-resistant nephrotic syndrome. Nat. Genet. 24, 349–354.
Chen, H., Charlat, O., Tartaglia, L.A., Woolf, E.A., Weng, X., Ellis, S.J., et al., 1996. Evidence that the diabetes gene encodes the leptin receptor: identification of a mutation in the leptin receptor gene in db/db mice. Cell 84, 491–495.
Cnop, M., Welsh, N., Jonas, J.C., Jorns, A., Lenzen, S., Eizirik, D.L., 2005. Mechanisms of pancreatic beta-cell death in type 1 and type 2 diabetes: many differences, few similarities. Diabetes 54 (Suppl. 2), S97–S107.
Datta, S.R., Brunet, A., Greenberg, M.E., 1999. Cellular survival: a play in three Akts. Genes Dev. 13, 2905–2927.
Diani, A.R., Sawada, G., Wyse, B., Murray, F.T., Khan, M., 2004. Pioglitazone preserves pancreatic islet structure and insulin secretory function in three murine models of type 2 diabetes. Am. J. Physiol. Endocrinol. Metab. 286, E116–E122.
Doublier, S., Salvidio, G., Lupia, E., Ruotsalainen, V., Verzola, D., Deferrari, G., et al., 2003. Nephrin expression is reduced in human diabetic nephropathy: evidence for a distinct role for glycated albumin and angiotensin II. Diabetes 52, 1023–1030.
Fornoni, A., Jeon, J., Varona Santos, J., Cobianchi, L., Jauregui, A., Inverardi, L., et al., 2010. Nephrin is expressed on the surface of insulin vesicles and facilitates glucose-stimulated insulin release. Diabetes 59, 190–199.
Garg, P., Verma, R., Nihalani, D., Johnstone, D.B., Holzman, L.B., 2007. Neph1 cooperates with nephrin to transduce a signal that induces actin polymerization. Mol. Cell. Biol. 27, 8698–8712.
George, B., Verma, R., Soofi, A.A., Garg, P., Zhang, J., Park, T.J., et al., 2012. Crk1/2-dependent signaling is necessary for podocyte foot process spreading in mouse models of glomerular disease. J. Clin. Invest. 122, 674–692.
Gerke, P., Huber, T.B., Sellin, L., Benzing, T., Walz, G., 2003. Homodimerization and heterodimerization of the glomerular podocyte proteins nephrin and NEPH1. J. Am. Soc. Nephrol. 14, 918–926.
Goldfine, A.B., Kulkarni, R.N., 2012. Modulation of β-cell function: a translational journey from the bench to the bedside. Diabetes Obes. Metab. 14, 152–160.
Hardt, P.D., Ewald, N., 2011. Exocrine pancreatic insufficiency in diabetes mellitus: a complication of diabetic neuropathy or a different type of diabetes? Exp. Diab. Res. 2011, 1–7.
Harita, Y., Kurihara, H., Kosako, H., Tezuka, T., Sekine, T., Igarashi, T., et al., 2009. Phosphorylation of nephrin triggers Ca^{2+} signaling by recruitment and activation of phospholipase C-{gamma}1. J. Biol. Chem. 284, 8951–8962.

Heikkila, E., Ristola, M., Havana, M., Jones, N., Holthofer, H., Lehtonen, S., 2011. Trans-interaction of nephrin and Neph1/Neph3 induces cell adhesion that associates with decreased tyrosine phosphorylation of nephrin. Biochem. J. 435, 619–628.
Hemmings, B.A., Restuccia, D.F., 2012. PI3K-PKB/Akt pathway. Cold Spring Harb. Perspect. Biol. 4, a011189.
Huber, T.B., Benzing, T., 2005. The slit diaphragm: a signaling platform to regulate podocyte function. Curr. Opin. Nephrol. Hypertens. 14, 211–216.
Huber, T.B., Kottgen, M., Schilling, B., Walz, G., Benzing, T., 2001. Interaction with podocin facilitates nephrin signaling. J. Biol. Chem. 276, 41543–41546.
Huber, T.B., Hartleben, B., Kim, J., Schmidts, M., Schermer, B., Keil, A., et al., 2003a. Nephrin and CD2AP associate with phosphoinositide 3-OH kinase and stimulate AKT-dependent signaling. Mol. Cell. Biol. 23, 4917–4928.
Huber, T.B., Simons, M., Hartleben, B., Sernetz, L., Schmidts, M., Gundlach, E., et al., 2003b. Molecular basis of the functional podocin-nephrin complex: mutations in the NPHS2 gene disrupt nephrin targeting to lipid raft microdomains. Hum. Mol. Genet. 12, 3397–3405.
Jeon, J., Leibiger, I., Moede, T., Walter, B., Faul, C., Maiguel, D., et al., 2012. Dynamin-mediated nephrin phosphorylation regulates glucose-stimulated insulin release in pancreatic beta cells. J. Biol. Chem. 287, 28932–28942.
Jones, N., Blasutig, I.M., Eremina, V., Ruston, J.M., Bladt, F., Li, H., et al., 2006. Nck adaptor proteins link nephrin to the actin cytoskeleton of kidney podocytes. Nature 440, 818–823.
Kestila, M., Lenkkeri, U., Mannikko, M., Lamerdin, J., McCready, P., Putaala, H., et al., 1998. Positionally cloned gene for a novel glomerular protein–nephrin–is mutated in congenital nephrotic syndrome. Mol. Cell 1, 575–582.
Khoshnoodi, J., Sigmundsson, K., Ofverstedt, L.G., Skoglund, U., Obrink, B., Wartiovaara, J., et al., 2003. Nephrin promotes cell-cell adhesion through homophilic interactions. Am. J. Pathol. 163, 2337–2346.
Kitsiou, P.V., Tzinia, A.K., Stetler-Stevenson, W.G., Michael, A.F., Fan, W.W., Zhou, B., et al., 2003. Glucose-induced changes in integrins and matrix-related functions in cultured human glomerular epithelial cells. Am. J. Physiol. Renal Physiol. 284, F671–F679.
Komori, T., Gyobu, H., Ueno, H., Kitamura, T., Senba, E., Morikawa, Y., 2008. Expression of kin of irregular chiasm-like 3/mKirre in proprioceptive neurons of the dorsal root ganglia and its interaction with nephrin in muscle spindles. J. Comp. Neurol. 511, 92–108.
Konstantinova, I., Nikolova, G., Ohara-Imaizumi, M., Meda, P., Kucera, T., Zarbalis, K., et al., 2007. EphA-ephrin-A-mediated beta cell communication regulates insulin secretion from pancreatic islets. Cell 129, 359–370.
Lahdenpera, J., Kilpelainen, P., Liu, X.L., Pikkarainen, T., Reponen, P., Ruotsalainen, V., et al., 2003. Clustering-induced tyrosine phosphorylation of nephrin by Src family kinases. Kidney Int. 64, 404–413.
Lehtonen, S., Zhao, F., Lehtonen, E., 2002. CD2-associated protein directly interacts with the actin cytoskeleton. Am. J. Physiol. Renal Physiol. 283, F734–F743.
Lenkkeri, U., Manikko, M., McCready, P., Lamerdin, J., Gribouval, O., Niaudet, P., et al., 1999. Structure of the gene for congenital nephrotic syndrome of the Finnish type (NPHS1) and characterization mutations. Am. J. Hum. Genet. 64, 51–61.
Li, H., Lemay, S., Aoudjit, L., Kawachi, H., Takano, T., 2004. SRC-family kinase Fyn phosphorylates the cytoplasmic domain of nephrin and modulates its interaction with podocin. J. Am. Soc. Nephrol. 15, 3006–3015.
Li, M., Armelloni, S., Ikehata, M., Corbelli, A., Pesaresi, M., Calvaresi, N., et al. 2011 Nephrin expression in adult rodent central nervous system and its interaction with glutamate receptors. J. Pathol. 225, 118–128.
Liu, X.L., Done, S.C., Yan, K., Kilpelainen, P., Pikkarainen, T., Tryggvason, K., 2004. Defective trafficking of nephrin missense mutants rescued by a chemical chaperone. J. Am. Soc. Nephrol. 15, 1731–1738.
Luo, X., Kraus, W.L., 2012. On PAR with PARP: cellular stress signaling through poly(ADP-ribose) and PARP-1. Genes Dev. 26, 417–432.
New, L.A., Chahi, A.K., Jones, N., 2013. Direct regulation of nephrin tyrosine phosphorylation by Nck adaptor proteins. J. Biol. Chem. 288, 1500–1510.
Palmen, T., Ahola, H., Palgi, J., Aaltonen, P., Luimula, P., Wang, S., et al., 2001. Nephrin is expressed in the pancreatic beta cells. Diabetologia 44, 1274–1280.
Patrakka, J., Tryggvason, K., 2007. Nephrin – a unique structural and signaling protein of the kidney filter. Trends Mol. Med. 13, 396–403.
Patrakka, J., Kestila, M., Wartiovaara, J., Ruotsalainen, V., Tissari, P., Lenkkeri, U., et al., 2000. Congenital nephritic syndrome (NPHS1): features resulting from different mutations in Finnish patients. Kidney Int. 58, 972–980.
Poitout, V., Stout, L.E., Armstrong, M.B., Walseth, T.F., Sorenson, R.L., Robertson, R.P. 1995 Morphological and functional characterization of beta TC-6 cells – an insulin-secreting cell line derived from transgenic mice. Diabetes 44 306–313.
Poitout, V., Olson, L.K., Robertson, R.P., 1996. Chronic exposure of betaTC-6 cells to supraphysiologic concentrations of glucose decreases binding of the RIPE3b1 insulin gene transcription activator. J. Clin. Invest. 97, 1041–1046.
Quack, I., Rump, L.C., Gerke, P., Walther, I., Vinke, T., Vonend, O., et al., 2006. 2006 beta-Arrestin2 mediates nephrin endocytosis and impairs slit diaphragm integrity. Proc. Natl. Acad. Sci. U.S.A. 103, 14110–14115.
Quack, I., Woznowski, M., Potthoff, S.A., Palmer, R., Konigshausen, E., Sivritas, S., et al., 2011. PKC alpha mediates beta-arrestin2-dependent nephrin endocytosis in hyperglycemia. J. Biol. Chem. 286, 12959–12970.
Rinta-Valkama, J., Palmen, T., Lassila, M., Holthofer, H., 2007. Podocyte-associated proteins FAT, alpha-actinin-4 and filtrin are expressed in Langerhans islets of the pancreas. Mol. Cell. Biochem. 294, 117–125.
Robertson, D., Savage, K., Reis-Filho, J.S., Isacke, C.M., 2008. Multiple immunofluorescence labelling of formalin-fixed paraffin-embedded (FFPE) tissue. BMC Cell Biol. 9, 13.
Ruotsalainen, V., Ljungberg, P., Wartiovaara, J., Lenkkeri, U., Kestila, M., Jalanko, H., et al., 1999. Nephrin is specifically located at the slit diaphragm of glomerular podocytes. Proc. Natl. Acad. Sci. U.S.A. 96, 7962–7967.
Schwarz, K., Simons, M., Reiser, J., Saleem, M.A., Faul, C., Kriz, W., et al., 2001. Podocin, a raft-associated component of the glomerular slit diaphragm, interacts with CD2AP and nephrin. J. Clin. Invest. 108, 1621–1629.
Shih, N.Y., Li, J., Cotran, R., Mundel, P., Miner, J.H., Shaw, A.S., 2001. CD2AP localizes to the slit diaphragm and binds to nephrin via a novel C-terminal domain. Am. J. Pathol. 159, 2303–2308.
Simons, M., Schwarz, K., Kriz, W., Miettinen, A., Reiser, J., Mundel, P., et al., 2001. Involvement of lipid rafts in nephrin phosphorylation and organization of the glomerular slit diaphragm. Am. J. Pathol. 159, 1069–1077.
Takahashi, H., Okamura, D., Starr, M.E., Saito, H., 2012. Age-dependent reduction of the PI3K regulatory subunit p85a suppresses pancreatic acinar cell proliferation. Aging Cell 11, 305–314.
Tossidou, I., Teng, B., Menne, J., Shushakova, N., Park, J.K., Becker, J.U., et al., 2010. Podocytic PKC-alpha is regulated in murine and human diabetes and mediates nephrin endocytosis. PLoS ONE 5, e10185.
Tryggvason, K., 1999. Unraveling the mechanisms of glomerular ultrafiltration: nephrin, a key component of the slit diaphragm. J. Am. Soc. Nephrol. 10, 2440–2445.
Tryggvason, K., Pikkarainen, T., Patrakka, J., 2006. Nck links nephrin to actin in kidney podocytes. Cell 125, 221–224.
Venieratos, P.D., Drossopoulou, G.I., Kapodistria, K.D., Tsilibary, E.C., Kitsiou, P.V., 2010. High glucose induces suppression of insulin signalling and apoptosis via upregulation of endogenous IL-1beta and suppressor of cytokine signalling-1 in mouse pancreatic beta cells. Cell. Signal. 22, 791–800.
Venkatareddy, M., Cook, L., Abuarquob, K., Verma, R., Garg, P., 2011. Nephrin regulates lamellipodia formation by assembling a protein complex that includes Ship2, filamin and lamellipodin. PLoS ONE 6, e28710.
Verma, R., Wharram, B., Kovari, I., Kunkel, R., Nihalani, D., Wary, K.K., et al., 2003. Fyn binds to and phosphorylates the kidney slit diaphragm component nephrin. J. Biol. Chem. 278, 20716–20723.
Verma, R., Kovari, I., Soofi, A., Nihalani, D., Patrie, K., Holzman, L.B., 2006. Nephrin ectodomain engagement results in Src kinase activation, nephrin phosphorylation, Nck recruitment, and actin polymerization. J. Clin. Invest. 116, 1346–1359.
Wagner, N., Morrison, M., Pagnotta, S., Michiels, J.-F., Schwab, Y., Tryggvason, K., et al., 2011. The podocyte protein nephrin is required for cardiac vessel formation. Hum. Mol. Genet. 20, 2182–2194.
Welsh, G.I., Saleem, M.A., 2010. Nephrin-signature molecule of the glomerular podocyte? J. Pathol. 220, 328–337.
Williams, J.A. 2010 Regulation of acinar cell function in the pancreas. Curr Opin. Gastroenterol. 26 478–483.
Yuan, H., Takeuchi, E., Taylor, G.A., McLaughlin, M., Brown, D., Salant, D.J., 2002. Nephrin dissociates from actin, and its expression is reduced in early experimental membranous nephropathy. J. Am. Soc. Nephrol. 13, 946–956.
Zhu, J., Sun, N., Aoudjit, L., Li, H., Kawachi, H., Lemay, S., et al., 2008. Nephrin mediates actin reorganization via phosphoinositide 3-kinase in podocytes. Kidney Int. 73, 556–566.